



NOVA
NOVA SCHOOL OF
SCIENCE & TECHNOLOGY

DEPARTMENT OF
PHYSICS

BEATRIZ VICENTE GUERREIRO

BSc of Science in Biomedical Engineering

THE ACUTE EFFECTS OF ACOUSTIC BIOFEEDBACK ON MUSCLE POWER

MASTER IN BIOMEDICAL ENGINEERING

NOVA University Lisbon
September, 2025



THE ACUTE EFFECTS OF ACOUSTIC BIOFEEDBACK ON MUSCLE POWER

BEATRIZ VICENTE GUERREIRO

BSc of Science in Biomedical Engineering

Adviser: Dr. Luís Miguel Domingues Ferreira Silva
Senior Researcher, NOVA School of Science and Technology

Co-adviser: Prof. Dr. José Miguel Bartolomeu de Mira
Assistant Professor, Egas Moniz School of Health and Science

Examination Committee

Chair: Prof. Dr. Susana Isabel dos Santos Silva Sérgio Venceslau
Assistant Professor, NOVA School of Science and Technology

Rapporteur: Prof. Dr. Valentina Borissovna Vassilenko
Assistant Professor, NOVA School of Science and Technology

Adviser: Dr. Luís Miguel Domingues Ferreira Silva
Senior Researcher, NOVA School of Science and Technology

The Acute Effects of Acoustic Biofeedback on Muscle Power

Copyright © Beatriz Vicente Guerreiro, NOVA School of Science and Technology, NOVA University Lisbon.

The NOVA School of Science and Technology and the NOVA University Lisbon have the right, perpetual and without geographical boundaries, to file and publish this dissertation through printed copies reproduced on paper or on digital form, or by any other means known or that may be invented, and to disseminate through scientific repositories and admit its copying and distribution for non-commercial, educational or research purposes, as long as credit is given to the author and editor.

To my grandparents who, unfortunately, could not accompany me in this stage of life. Avó Joana e Avô Francisco, onde quer que estejam, continuarei a lutar sempre por mais, levando comigo a força e a sabedoria que me deixaram.

ACKNOWLEDGEMENTS

First, I would like to express my sincere gratitude to Professor Luís Silva for his guidance, knowledge, and encouragement throughout this journey, always demonstrating a deeply human side. My deepest thanks also go to Dania, for always understanding me so well, guiding me, and helping me whenever I needed it, without hesitation. I also thank Professor José Mira for kindly dedicating his time to the detailed revision of this document, providing valuable feedback that greatly contributed to its improvement.

To my family, words will never be enough. To my Mom, Dad and brother: you are my safe harbor. Without your unconditional love, it would have been impossible to keep going when strength seemed to fade. Thank you for always believing in me and encouraging me to pursue my dreams. To Avó Maria, Avô Horácio, Tia Ana, Tio Luís, Tia Florbela, Prima Marta e Primo Diogo: thank you for your encouraging words and for showing such pride in me.

A very special thank you to my boyfriend, Rafael. You have been by my side since the very beginning of this journey. Your support, in ways I can hardly put into words, has meant everything to me. You were always the first to cheer me on, through both highs and lows, constantly reminding me of my worth even when I doubted myself.

To my lifelong girls, you know who you are: thank you for standing beside me during my growth. To my university friends, BioSaídas, who I know I will carry with me for life: you are incredible. Together we faced the best and worst moments of college, and your support was fundamental during the most challenging times. To my godmother Adriana, who has accompanied me almost since my very first day: thank you for the countless messages, voice notes, and advice. Life was generous when it placed you in my path. I would also like to express my gratitude to Mr. Afonso and Bruno, for their contagious joy and daily encouragement during the preparation of this work.

To all, my heartfelt thanks for being part of this journey.

ABSTRACT

Muscle power training is often avoided in vulnerable populations, such as older adults, due to safety concerns associated with explosive movements. Yet, the age-related decline in muscle power, a condition known as powerpenia, represents the earliest and most critical loss of muscular function, increasing the risk of falls.

To address the challenge of safely delivering power training to those who need it most, Acoustic Biofeedback (ABF) derived from muscle electrical activity can be leveraged to guide training that targets muscle power.

This study aimed to investigate the acute effects of electromyography (EMG)-based ABF on muscle power in young adults, assessing the feasibility of the tool, as an initial step toward its application in aging populations. Twenty-four healthy participants performed a power test with bench press and squat exercises at multiple relative loads across three sessions, under two auditory conditions: ABF and generic Gym Music (GM). Power-related and EMG-derived metrics were extracted, complemented by participants' subjective enjoyment of the power test under both stimuli.

Results showed that ABF elicited short-term improvements in men's bench press performance, particularly in Maximum Power ($BF_{-0} = 19.31$) and Maximum Velocity ($BF_{-0} = 9.198$), whereas women displayed stable values largely influenced by physical activity level rather than stimulus type. Intramuscular coordination of upper and lower limbs did not change over sessions but revealed clear sex-related disparities. Although perceived enjoyment was higher with GM in both sexes, only ABF demonstrated acute performance advantages.

These findings support EMG-based ABF as a promising aid for power-oriented training, suggesting that longer interventions could elicit further beneficial adaptations in muscular power output.

Keywords: Powerpenia, Muscle Power, High-Velocity Training, ABF, EMG

RESUMO

O treino de potência muscular é frequentemente evitado em populações vulneráveis, como os idosos, devido ao risco de segurança associado a movimentos explosivos. No entanto, o declínio da potência muscular, uma condição designada de *powerpenia*, representa a perda mais precoce e crítica da função muscular, aumentando o risco de quedas.

Para ultrapassar o desafio de promover treino de potência de forma segura a quem mais necessita, o Biofeedback Acústico (ABF), derivado da atividade elétrica muscular, pode ser utilizado para orientar o treino direcionado à potência muscular.

Este estudo investigou os efeitos agudos do ABF baseado em Eletromiografia (EMG) na potência muscular em jovens adultos, avaliando a sua viabilidade, como primeiro passo para aplicação em populações idosas. Vinte e quatro participantes realizaram um teste de potência com exercícios de supino e agachamento, em várias cargas relativas e ao longo de três sessões, sob duas condições auditivas: ABF e Música de Ginásio (GM). Foram extraídas métricas de potência e de EMG, complementadas pelo nível de satisfação percebido com o teste de potência em relação aos dois estímulos.

Os resultados mostraram que o ABF provocou melhorias de curto prazo no desempenho do supino nos homens, particularmente na Potência Máxima ($BF_{-0} = 19.31$) e na Velocidade Máxima ($BF_{-0} = 9.198$), enquanto as mulheres apresentaram valores estáveis ao longo das sessões, influenciados principalmente pelo nível de atividade física e não pelo tipo de estímulo. A coordenação intramuscular dos membros superiores e inferiores não se alterou ao longo das sessões, mas revelou disparidades claras entre sexos. Embora a percepção de satisfação tenha sido superior com a GM em ambos os sexos, apenas o ABF demonstrou vantagens agudas de desempenho.

Estes resultados apoiam o ABF baseado em EMG como uma ferramenta promissora para o treino de potência muscular, sugerindo que intervenções mais prolongadas poderão induzir adaptações benéficas adicionais para a produção de potência muscular.

Palavras-chave: *Powerpenia*, Potência Muscular, Treino de Alta Velocidade, ABF, EMG

CONTENTS

List of Figures	x
List of Tables	xii
Abbreviations	xiv
1 Introduction	1
1.1 Motivation	1
1.2 Objectives	2
2 Theoretical Concepts	3
2.1 Force Manifestations	3
2.1.1 Maximal Strength	3
2.1.2 Rapid Force	3
2.1.3 Rate of Force Development	3
2.1.4 Skeletal Muscle Power	4
2.2 Sarcopenia and Dynapenia	4
2.3 Powerpenia	5
2.4 Muscle Power Training	5
2.5 Acoustic Biofeedback	5
3 Literature Review	6
3.1 Muscle Power Across the Lifespan	6
3.2 Determinants of Muscle Power Decline	7
3.3 Functional Relevance of Muscle Power	7
3.4 Training Evidence: Muscle Power Training as a More Effective Strategy than Strength Training	7
3.5 Neural and Muscular Adaptations to Muscle Power Training	8
3.6 Acoustic Biofeedback	8
4 Methods	10

4.1	Study Type	10
4.2	Data Collection and Protocol	10
4.2.1	Participants	10
4.2.2	Instrumentation and Equipment	11
4.2.3	Baseline Session	12
4.2.4	Experimental Procedure	13
4.3	Signal Processing	15
4.3.1	Units Conversion	15
4.3.2	ACC Filtering	15
4.3.3	Load Cell Filtering	16
4.3.4	Velocity Filtering	16
4.3.5	Power Filtering	16
4.3.6	EMG Filtering	16
4.4	Algorithms	17
4.4.1	Concentric Phase Detection Algorithm	17
4.4.2	Repetition Start Detection Algorithm	17
4.4.3	EMG Onset Detection Algorithm	18
4.5	Metrics	19
4.5.1	Maximum Velocity	19
4.5.2	Maximum Power	20
4.5.3	Velocity Power Difference	20
4.5.4	Correlation of Repetition Profiles	20
4.5.5	Peak Velocity and Peak Power Index	20
4.5.6	Peak Rate of Power Development	21
4.5.7	Window and Total Power Slopes	21
4.5.8	EMG Onset to Peak Power	21
4.5.9	EMG Rise Time and Slope	21
4.5.10	EMG Median Frequency	22
4.6	Data Organization and Database Structure	22
4.7	Statistical Analysis	23
4.7.1	Full-Sample Analysis	23
4.7.2	Sex-Specific Analysis	24
5	Results	26
5.1	Overall Analysis Across Participants	26
5.2	Sex-Specific Analysis	29
5.2.1	Male Participants Analysis	30
5.2.2	Female Participants Analysis	32
5.3	Perceived Enjoyment with Auditory Stimuli	34
6	Discussion	35

6.1	Overall Analysis: Progression and Sex Differences	35
6.1.1	Bench Press: Sex-Based Performance Disparities	36
6.1.2	Squat: Sex-Based Performance Disparities	37
6.2	Adaptation Analyses	38
6.3	Limitations	39
7	Conclusions and Future Work	40
	Bibliography	41
	Appendices	
A	Informed Consent	53
B	Submaximal Test for 1RM Estimation	57
B.1	Maximal Strength Assessment	57
C	Experimental Protocol	59
C.1	Preparation (2 min)	59
C.2	Placement of Instruments (10 min)	59
C.2.1	Required Materials and Connection to BioPlux	59
C.2.2	Skin Preparation	60
C.2.3	Sensor Placement	60
C.2.4	ACC and Load Cell	62
C.2.5	Connection to the BioPlux	62
C.3	Resting Measurements (2 min)	63
C.4	Start of Training	63
C.4.1	Required Training Materials	63
C.4.2	Activation (10 min)	63
C.4.3	Training Plan (50 min)	64
C.5	Correct Execution of the Exercises	65
C.5.1	Squat	65
C.5.2	Bench Press	66
C.6	Stretching	66
C.7	Cool-Down (4 min)	67
C.7.1	Walking	67
C.7.2	Rest	67
C.8	Equipment Removal (10 min)	68
C.9	Enjoyment Assessment (3 min)	68
D	Experimental Session	69
E	Event Detection Algorithms and EMG Processing	70

LIST OF FIGURES

2.1	Fundamental muscle performance relationships. Adapted from [11].	4
4.1	Equipment and sensor setup for signal acquisition.	14
4.2	Directory structure for participant data storage.	23
5.1	Descriptive plots of the variables most influenced by Session and Gender, highlighting their progressive evolution across sessions in the bench press exercise. S = Session; 1 = Male, 2 = Female.	28
5.2	Descriptive plots of the variables most influenced by Session and Gender, highlighting their progressive evolution across sessions in the squat exercise. S = Session; 1 = Male, 2 = Female.	29
5.3	Evolution of EMG Rise Time across sessions in the bench press for women.	33
5.4	PACES-8 scores comparing perceived enjoyment between the ABF and GM auditory stimuli, stratified by sex. 1- Male; 2- Female.	34
C.1	Sensor arrangement in the BioPlux device.	60
C.2	EMG – Triceps Brachii.	61
C.3	EMG – Vastus Lateralis.	61
C.4	Recommended ECG electrode positions.	62
C.5	Shoulder rotation. Adapted from [70].	64
C.6	Squat – <i>Speediance</i> . Adapted from [70].	66
C.7	Bench Press – <i>Speediance</i> . Adapted from [70].	66
C.8	Stretching. Adapted from [70].	67
D.1	Experimental Session.	69
E.1	Concentric Phase Detection Algorithm.	70
E.2	Repetition Start Detection Algorithm.	70
E.3	Application of the Teager-Kaiser Energy Operator (TKEO).	71
E.4	Rectification and Gaussian smoothing used to obtain a stable EMG activation envelope.	71

E.5 EMG Onset Detection Algorithm.	71
--	----

LIST OF TABLES

4.1	Sample characteristics by gender.	11
4.2	Parameters used in the Concentric Phase Detection Algorithm.	17
4.3	Parameters used in the Repetition Start Detection Algorithm.	18
4.4	Parameters used in the EMG Onset Detection Algorithms.	19
5.1	Bayesian repeated-measures ANOVA results for all evaluated metrics in the bench press exercise.	26
5.2	Bayesian repeated-measures ANOVA results for all evaluated metrics in the squat exercise.	28
5.3	Bayesian repeated-measures ANOVA results for all evaluated metrics in the bench press exercise among male participants.	30
5.4	Bayesian repeated-measures ANOVA results for all evaluated metrics in the squat exercise among male participants.	31
5.5	Bayesian repeated-measures ANOVA results for all evaluated metrics in the bench press exercise among female participants.	32
5.6	Bayesian repeated-measures ANOVA results for all evaluated metrics in the squat exercise among female participants.	33
B.1	Coefficients of prediction of 1RM based on the number of repetitions. Adapted from Baechle & Groves (1992).	58
C.1	ECG lead configuration.	62
C.2	Bench press protocol based on estimated 1RM values.	64
C.3	Squat protocol based on estimated 1RM values.	65
F.1	Bayesian repeated-measures ANOVA model comparison for Maximum Power in the bench press (overall analysis).	72
F.2	Bayesian repeated-measures ANOVA model comparison for Maximum Velocity in the bench press (overall analysis).	72
F.3	Bayesian repeated-measures ANOVA model comparison for Peak RPD in the bench press (overall analysis).	73

F.4	Bayesian repeated-measures ANOVA model comparison for EMG Rise Time in the bench press (overall analysis).	73
F.5	Bayesian repeated-measures ANOVA model comparison for Maximum Power in the squat (overall analysis).	73
F.6	Bayesian repeated-measures ANOVA model comparison for Peak RPD in the squat (overall analysis).	74
F.7	Bayesian repeated-measures ANOVA model comparison for Power Peak Index in the squat (overall analysis).	74
F.8	Bayesian repeated-measures ANOVA model comparison for Maximum Power in the bench press (sex-specific analysis: men).	74
F.9	Bayesian repeated-measures ANOVA model comparison for Maximum Velocity in the bench press (sex-specific analysis: men).	75
F.10	Bayesian repeated-measures ANOVA model comparison for Maximum Power in the squat (sex-specific analysis: men).	75
F.11	Bayesian repeated-measures ANOVA model comparison for Peak RPD in the squat (sex-specific analysis: men).	75
F.12	Bayesian repeated-measures ANOVA model comparison for EMG rise time in the bench press (sex-specific analysis: women).	76

ABBREVIATIONS

1RM	One Maximum Repetition (<i>pp. 3, 7, 8, 13, 14, 36, 57, 64</i>)
ABF	Acoustic Biofeedback (<i>pp. 1–3, 5, 8–10, 12, 14, 22, 24, 25, 31–35, 38–40, 65</i>)
ACC	Acceleration (<i>pp. 12, 15, 59, 63</i>)
ACSM	American College of Sports Medicine (<i>pp. 14, 65</i>)
CSA	Cross-Sectional Area (<i>pp. 5, 36</i>)
ECG	Electrocardiography (<i>pp. 12, 13, 59, 62, 63</i>)
EMG	Electromyography (<i>pp. 2, 8, 9, 12, 13, 15, 16, 18, 19, 21, 22, 27, 29–38, 40, 59–61, 63</i>)
GM	Gym Music (<i>pp. 2, 11, 14, 22, 25, 31–35, 38, 40, 65</i>)
IPAQ	International Physical Activity Questionnaire (<i>pp. 11, 24</i>)
MHC	Myosin Heavy Chain (<i>p. 8</i>)
MPT	Muscle Power Training (<i>pp. 3, 6–9</i>)
PACES-8	Physical Activity Enjoyment Scale, Portuguese 8-item version (<i>pp. 10–12, 34, 68</i>)
RFD	Rate of Force Development (<i>pp. 3, 4, 37</i>)
RPD	Rate of Power Development (<i>pp. 21, 27–33, 36–38</i>)
sEMG	Surface Electromyography (<i>pp. 9, 39</i>)
ST	Strength Training (<i>pp. 7, 8</i>)
STL	Seasonal-Trend decomposition using Loess (<i>p. 16</i>)
TKEO	Teager-Kaiser Energy Operator (<i>p. 18</i>)

VL Vastus Lateralis (*pp. 13, 37–39*)

INTRODUCTION

1.1 Motivation

Muscle power training is commonly associated with athletes, where explosive performance is crucial. By contrast, it is less often considered for elderly individuals or those with neuromuscular diseases, largely due to concerns about safety and the assumption that they are unable to perform explosive efforts. As a result, current guidelines tend to limit these populations to low-intensity and long-duration endurance exercises [2].

However, aging and disease are accompanied by profound declines in muscle functionality [3], including sarcopenia (loss of muscle mass), dynapenia (loss of muscle strength), and powerpenia (loss of muscle power). Among these, muscle power is the most critical to address, as powerpenia precedes the other losses and shows the steepest decline [4]. Degenerative changes at the neuromuscular junction [5], together with a progressive shift from fast-twitch to slow-twitch fibers, further explain this vulnerability. Since fast and powerful movements are essential to prevent falls, the loss of power becomes a key determinant of functional decline [6].

The challenge lies in safely delivering power training to fragile populations who need it most. Here, sensory feedback may play a key role by leveraging the human ability to follow sounds and adapt motor output accordingly, a process known as sensorimotor integration [7].

This study aims to test an innovative solution within a power test protocol by applying Acoustic Biofeedback (ABF) of the muscle response in a young population. As a training aid, ABF could enable real-time corrections in muscle activation to better target muscle power, that may improve exercise safety. This work is part of the ASTROPOWER project [8], which explores the analogy between aging and microgravity adaptations to develop new strategies against muscle power loss.

1.2 Objectives

Given the need to develop training strategies that combat muscle power loss and can be safely and effectively applied to vulnerable populations, such as the elderly, the first step is to evaluate the feasibility in a healthy cohort to establish a reference. Accordingly, the main objective of this work is to investigate the acute effects of Electromyography (EMG)-based ABF on muscle power in young individuals, who serve as a benchmark for the healthy population.

To ensure the success of this work, the following objectives must be attained:

1. To investigate whether ABF acutely influences muscle power production compared to ordinary Gym Music (GM) in both males and females.
2. To investigate differences in intramuscular coordination of the upper and lower limbs under both stimuli in males and females.
3. To evaluate the perceived exercise enjoyment of males and females when exposed to ABF versus GM.

Since long-term adaptations result from both acute and chronic effects, this study first sought to determine whether acute adaptations could be elicited with ABF. Demonstrating short-term changes provides initial evidence that, if continued, this approach may also promote long-term benefits, supporting its potential as a novel strategy to counteract powerpenia.

The research work described in this dissertation was carried out in accordance with the norms established in the ethics code of Universidade Nova de Lisboa. The work described and the material presented in this dissertation, with the exceptions clearly indicated, constitute original work carried out by the author.

In the present work, generative artificial intelligence tools, namely ChatGPT-5, were employed for text reformulation, and for code debugging. These tools were used under the supervision of the author, and all generated content was verified for accuracy. The authorship and validation of the content remain entirely the responsibility of the author, and the use of artificial intelligence is in full compliance with institutional standards of academic integrity.

THEORETICAL CONCEPTS

This chapter introduces the theoretical foundations of the study, addressing the different manifestations of muscle force and the concept of powerpenia. It further considers Muscle Power Training (MPT) and the use of the ABF.

2.1 Force Manifestations

2.1.1 Maximal Strength

Maximal strength is the highest force value that the neuromuscular system can produce in a single voluntary contraction against an resistance, regardless of the time needed to produce it [9]. Maximal intensity is one of the characteristics of maximal strength and refers to the highest effort that the body can produce, usually assessed through One Maximum Repetition (1RM) tests, where the goal is to lift the heaviest possible load only once [10]. It is a quantity expressed in *Newton (N)*. Maximal strength is considered the basis for the other manifestations of strength, namely rapid force and strength endurance [9].

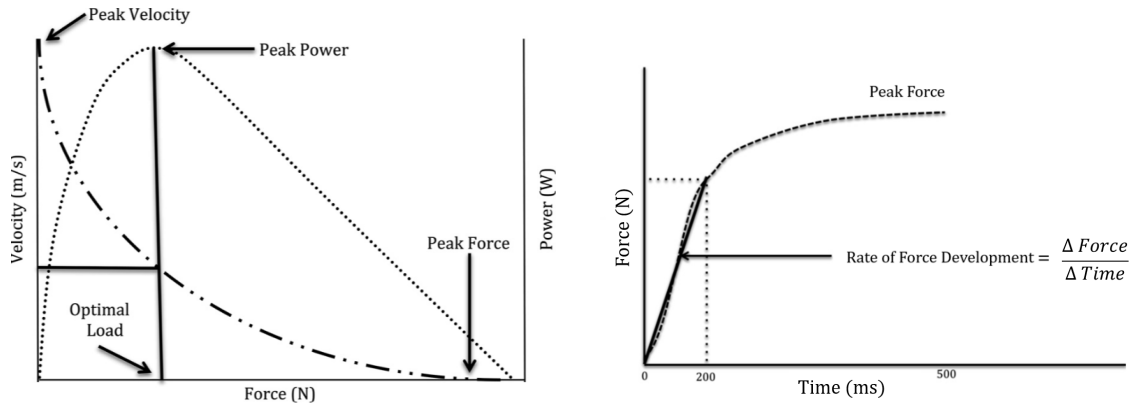
2.1.2 Rapid Force

Rapid force is the ability of the neuromuscular system to generate the greatest impulse in a limited time interval [9]. During concentric contractions, increasing movement speed reduces the muscle's ability to generate force, limiting the external resistance that can be overcome (Figure 2.1a) [9]. At slower speeds, force production is greater due to more time for motor unit recruitment. This reflects mechanical and neuromuscular limits in fast actions. Thus, two important expressions of rapid force become relevant: Rate of Force Development (RFD) and skeletal muscle power.

2.1.3 Rate of Force Development

The RFD is defined as the production of force per unit of time [9] and is therefore a measure of how quickly the muscle produces force during a contraction. It is calculated

from the slope of the force versus time curve, as shown in Figure 2.1b, and is expressed in Ns^{-1} [9]. It is particularly important in activities that require explosive movements and rapid responses to stimuli [2].



(a) Relationship between force, velocity and power.

(b) Relationship between force and time, highlighting the Rate of Force Development.

Figure 2.1: Fundamental muscle performance relationships. Adapted from [11].

2.1.4 Skeletal Muscle Power

Muscle power is the amount of work done per unit of time, determined by the product of force and velocity (the speed at which that force is applied) [12]. Muscle power is expressed in *Watt* (W) and can be modulated by changes in force, velocity, or both [9].

To generate force quickly at relatively high speeds, three aspects must be considered: developing maximal strength to increase force production, improving the RFD to accelerate force generation, and balancing force with velocity when performing high-speed shortening contractions.

Muscle power is mainly determined by the composition of muscle fiber types, muscle strength/mass and the level of neuromuscular activation during exercise [13].

2.2 Sarcopenia and Dynapenia

Sarcopenia is a condition characterized by gradual loss of muscle mass, observed with age [14]. This process begins around the age of 40, with more significant muscle loss in the following decades [15]. Several factors contribute to this decline, including hormonal changes, decreased physical activity, and changes in protein synthesis [16].

Dynapenia is the age-related loss of muscle strength that is not caused by neurological or muscular diseases. Recent studies suggest that the origin of this loss is related to subclinical deficits in the structure and function of the nervous system and/or changes in the intrinsic force-generating properties of skeletal muscle [17].

2.3 Powerpenia

The concept of powerpenia has recently been introduced to describe the loss of skeletal muscle power across one's lifespan, but also for clinical conditions and/or physical inactivity. It highlights muscle power as an important biomarker of healthy aging [4].

The loss of power is due in part to the muscle loss and atrophy that occurs, with a reduction in Cross-Sectional Area (CSA) of type II muscle fibers, which can generate four times more power than type I fibers [18]. This is because type II fibers are used less frequently in daily activities and are more prone to atrophy due to disuse.

In addition, decreased motor unit recruitment and firing rates, increased coactivation and decreased coordination of muscle groups, and a slowing of nerve conduction velocity are all factors that contribute to the power deficit [19].

2.4 Muscle Power Training

Muscle Power Training is one of the key components of physical conditioning in older adults. It is a form of exercise designed to improve muscle efficiency and the ability to generate force quickly [16].

While high force at low velocity or high velocity at low force results in less power production, peak power occurs at a balance between force and velocity [9]. This balance allows the muscle to contract at a velocity that produces the most work in the shortest time, maximizing power.

However, in the velocity-power relationship (see Figure 2.1), power production initially increases as speed increases, reaches a peak, and then decreases as speed increases. At high speeds, muscle force is too low to maintain high power output, leading to a decrease in total power [9].

Therefore, it is important to balance speed and load in exercises to achieve maximum power production, with the concentric phase emphasized to maximize movement velocity [10].

2.5 Acoustic Biofeedback

ABF is a cognitive assistance technique that uses sound signals to provide the individual with real-time information on physiological processes. It is a process by which the nervous system processes sensory input and adjusts motor output. The characteristics of the bioelectrical signal are mapped to the characteristics of the sound signal through various conversion components that must be considered to create comfortable and intuitive sound feedback [20]. In this study, ABF is based on muscle electrical activity and may enhance the independence of older adults, during power training, by helping them consciously adjust their behavior and perform exercises correctly without constant supervision.

LITERATURE REVIEW

This chapter reviews the literature on the key concepts underlying muscle power and its decline with aging, highlights MPT as a preferred approach, and examines current methods for its assessment together with the emerging role of auditory biofeedback.

3.1 Muscle Power Across the Lifespan

Aging entails a progressive neuromuscular decline [21], traditionally described by sarcopenia and dynapenia biomarkers [22]. However, recent evidence highlights muscle power loss as a more sensitive marker of functional performance [23], since it reflects not only strength but also the capacity to generate force rapidly, a key requirement for many daily activities [24].

Several studies emphasize that muscle power declines earlier and more rapidly than muscle strength or mass. Evidence from healthy adults across a wide age range shows that muscle power begins to decline as early as the third to fourth decade of life [25]. In older adults, this decline accelerates and reaches an estimated rate of 3–4% per year [19]. It is essential to identify the specific life stages at which this decline begins, given that detecting such critical periods may enable earlier interventions to prevent functional loss in older age. Evidence from large cohort studies suggests that this decline follows a curvilinear pattern, accelerating with advancing age [25]. Lower limb muscle power tends to increase during growth, reaching its peak between 20 and 30 years of age in healthy, untrained adults [26]. It remains relatively stable until around the age of 40, after which it enters a phase of progressive and linear decline [25]. Importantly, muscle power relative to body mass appears to be more relevant for daily functional performance than absolute power [27], with its determinants varying across the lifespan and between sexes. In this regard, Alcazar et al. [21] reported that, in healthy adults, relative muscle power decreases with age, starting after 40 due to reduced specific power and increased body mass, and after 70 as a result of declines in both specific power and leg lean mass. More recently, Wiegmann et al. [28] reported, in a large cohort of adults aged 20–90, that muscle power showed the earliest and steepest decline across age groups, beginning in early adulthood,

while reductions in strength and mass appeared later. While the timing of decline is important, understanding the mechanisms underlying this loss is equally critical.

3.2 Determinants of Muscle Power Decline

Early decline in muscle power is linked to several age-related neuromuscular changes [29]. With age, there is a reduction in the number of large, fast-conducting myelinated motor axons, due to demyelination and increased internodal distances [30]. These changes lead to less effective neural transmission and delayed motor response, as reported by Vandervoort et al. [31]. In addition to altered neural conduction, aging is also associated with greater coactivation of antagonist muscles during walking [32], [33]. According to Monaco et al. [34], this may function as a compensatory mechanism to increase joint stability but reduces net torque and, consequently, muscle power output. Furthermore, morphological changes at the neuromuscular junction occur throughout life. There is a selective reduction in type II fast fibers [35], which are more vulnerable to the denervation process and are often reinnervated by type I motor neurons. This process promotes a predominance of slow fibers and compromises excitability and the ability to generate rapid responses [5].

3.3 Functional Relevance of Muscle Power

Beyond its decline, the functional relevance of muscle power must also be emphasized. Evidence indicates that muscle power is more closely associated with independence in daily life than maximal strength or muscle mass. Suzuki et al. [36] showed that ankle flexor power was a stronger predictor of functional performance than strength in tasks such as repeated chair stands and stair climbing. Similarly, Cuoco et al. [37] demonstrated that lower-limb power, particularly at 40% 1RM, was the best predictor of habitual gait speed and showed stronger associations with stair climbing and chair rise than maximal strength. These findings highlight powerpenia as a more sensitive and functionally relevant predictor of musculoskeletal impairment than either dynapenia or sarcopenia.

3.4 Training Evidence: Muscle Power Training as a More Effective Strategy than Strength Training

For several years, Strength Training (ST) has been defined as an important strategy for preventing or delaying physical decline. However, this type of training primarily recruits slow-twitch fibers, which are less effective for developing the rapid force production required for muscle power. To address this limitation, MPT has been proposed, as it has been shown to provide greater improvements in skeletal muscle power than traditional low velocity ST [3].

Research findings from intervention studies support this. Bottaro et al. [38] compared 10 weeks of power training (fast movements at 60% 1RM) with traditional ST (slow execution) in older inactive men (60–76 years). While both groups increased maximal strength, the power training group achieved superior gains in muscle power and functional performance. Similarly, Orr et al. [39] found greater improvements in dynamic balance with high-velocity resistance training compared to an inactive control group, particularly when training at low intensity (20% 1RM). Miszko et al. [40] also showed that high-speed training at 40% 1RM led to greater improvements in global functional capacity than traditional resistance training. Together, these studies show that power-focused training is more effective than traditional ST at improving function in older adults.

Although most research has focused on older adults, examining younger populations helps clarify the role of muscle power in performance earlier in life. Robust evidence in youth shows that power training improves jump performance, velocity, and overall power capacity [41]. Dorrell et al. [42] reported that, in trained young men, six weeks of velocity-based training produced similar or superior gains in maximal strength and increased vertical jump height, whereas traditional percentage-based training did not. On the same topic, Sekulović et al. [43] found that in elite young soccer players, training with a 15% velocity loss threshold produced comparable strength gains but superior improvements in vertical jump, reactive strength index, and agility compared to traditional ST or training with 30% of velocity loss.

3.5 Neural and Muscular Adaptations to Muscle Power Training

The effects observed with MPT are likely not due to changes in body composition (i.e., muscle hypertrophy), but rather to neural adaptations [44]. Regulation may occur at multiple levels of the neuromuscular system, ranging from central motor control to the muscle fibers [45]. Van Cutsem et al. [46] reported that MPT modified muscle fiber behavior, with fibers displaying faster contractile properties, as evidenced by an increased doublet discharge rate. In line with this, Liu et al. [47] compared two bench press protocols (3RM vs. 10 fast concentric repetitions at 30% 1RM) in men and observed that high-velocity training promoted a shift from Myosin Heavy Chain (MHC)-I to MHC-IIa fibers. These findings suggest that MPT may facilitate the transition from slow-to fast-twitch fibers.

Despite evidence for MPT as an effective strategy against age-related functional decline, concerns remain about its safety in older adults [48]. This study proposes an ABF-based approach that sonifies EMG activity into real-time auditory cues to support MPT.

3.6 Acoustic Biofeedback

Studies have consistently demonstrated that auditory stimuli, even in their basic forms, can modulate muscle activity and performance, providing the foundation for more advanced feedback systems like ABF. Jaskowski et al. [49] demonstrated in a reaction time task that

force output increased proportionally with stimulus intensity only under auditory, but not visual conditions. In a sport-specific context, Murgia et al. [50] tested auditory cues linked to the lifting phases of the bench press (low-intensity sound in the eccentric phase, high-intensity in the concentric). While peak power did not differ, average power was higher in the auditory condition, suggesting that auditory input facilitates the expression of athletes' full potential. Beyond strength and power, motor learning studies have shown that auditory feedback leads to greater improvements than visual feedback [51] and enhances postural control [52].

Beyond simple auditory stimulation, structured biofeedback systems have been developed and applied across different contexts. Lorenzoni et al. [53] evaluated a music-based biofeedback system during deadlifts, where correct movements triggered high-quality sounds and incorrect executions produced distortions. They found it as effective as verbal coaching for improving technique and motivation, supporting sonification as a valid tool for safe and technology-assisted training. In the domain of balance, Chiari et al. [54] developed a prototype converting trunk accelerations into stereo sounds, which enhanced stability in healthy adults, particularly under challenging conditions. More recently, Lyons et al. [55] applied auditory feedback based on ankle plantarflexion velocity in older adults, finding that it promoted more efficient gait by increasing ankle contribution to propulsion and reducing hip reliance.

While these systems rely on external measures such as motion or force, other approaches have explored direct EMG sonification. To date, however, there is no standardized approach for mapping EMG into sound. Pauletto et al. [7] conducted an experiment using amplitude modulation of EMG signals to generate timbres, finding that participants could meaningfully associate sounds with natural gestures (e.g., breathing, ocean waves), supporting the effectiveness of auditory EMG representation. Nakayama et al. [56] proposed a real-time system for detecting and sonifying smiles via EMG signals, reporting higher comprehensibility and pleasantness compared to visual or no feedback. Peres et al. [57] further demonstrated that tailoring pitch and intensity of Surface Electromyography (sEMG) sonification optimized participants' ability to estimate muscle activation timing, strongly suggesting that EMG sonification design should be task specific. Collectively, these findings support EMG-based sonification as a viable and intuitive method for representing muscle activity.

Its application has been shown clinical benefits, improving gait in stroke and cerebral palsy patients [58], [59] and enhancing knee mobility after surgery [60]. In young adults, Yang et al. [61] combined EMG with kinematic data to provide auditory feedback during biceps curls, which improved performance and reduced fatigue. In addition, Tsubouchi et al. [20] reported that frequency- or rhythm-based sonification enabled participants to correctly recognize EMG activity patterns in over 80% of cases, outperforming conventional visual feedback. In this way, the present study takes advantage of the EMG-based ABF's potential to improve the effectiveness and safety of MPT.

METHODS

This chapter describes the methodology adopted in this study. It begins by defining the study type, followed by a detailed description of data collection procedures, including participant recruitment and characteristics, materials used, and the experimental protocol. Subsequent sections describe the signal processing steps, developed algorithms, and the extracted metrics. Finally, the organization and structure of the resulting database are outlined.

4.1 Study Type

This study follows a cross-sectional design, focusing on the acute responses to two distinct auditory stimuli. Although each participant completed three sessions, these were scheduled to familiarize participants with the protocol, increase measurement reliability, and reduce the influence of random factors. Within this exploratory approach, the study aimed to investigate the effect of muscle sonification on muscle power production during a power test performed at different loads. The study was conducted in a young population in order to assess the feasibility and usability of the ABF tool. This initial stage therefore lays the groundwork for future longitudinal research in elderly populations.

4.2 Data Collection and Protocol

4.2.1 Participants

A total of 24 participants (12 males and 12 females) were recruited for this study, most of whom were students from Faculdade de Ciências e Tecnologias da Universidade Nova de Lisboa, with two participants from another institution. Their characteristics are presented in Table 4.1. The sample size was determined a priori using G*Power (version 3.1) [62], which indicated a minimum of 20 participants ($f = 0.3$, $\alpha = 0.05$, power = 0.80). Considering possible dropouts, the sample size was increased to 24.

In addition to anthropometric and maximal strength variables, Physical Activity Enjoyment Scale, Portuguese 8-item version (PACES-8) [63] [64] and the short version of

the International Physical Activity Questionnaire (IPAQ) [65] were applied with scores calculated according to official protocols [66] [67]. PACES-8 scores (with a range of 8–56; higher values indicating greater enjoyment) were similar across conditions and between genders, with slightly higher values observed under GM. Regarding the IPAQ, most participants were classified as having a moderate to high level of physical activity.

All individuals received a detailed explanation of the study’s objective and experimental protocol before being included in the study and signed an informed consent form (see Appendix A). Sessions were scheduled flexibly in coordination with each participant to ensure their comfort and availability. This study was conducted as part of the ASTROPOWER project, and the experimental protocol was approved by the Ethics Committee of Faculdade de Ciências e Tecnologias da Universidade Nova de Lisboa (CE_FCT_021-2025).

Table 4.1: Sample characteristics by gender.

Variables	Male (N=12)	Female (N=12)	Total (N=24)
Age (years)	21.2 ± 2.1	23.2 ± 1.9	22.2 ± 2.2
Body mass (kg)	78.2 ± 11.1	56.3 ± 3.5	67.2 ± 13.8
Body fat (%)	16.1 ± 5.2	26.3 ± 4.9	21.2 ± 7.2
Lean mass (%)	62.1 ± 7.9	39.3 ± 2.4	50.7 ± 13.0
Height (m)	1.78 ± 0.07	1.60 ± 0.04	1.69 ± 0.11
Handgrip strength (kg)	41.2 ± 8.7	26.4 ± 6.3	33.8 ± 10.6
1RM Bench press (kg)	60.8 ± 15.9	25.6 ± 5.3	43.2 ± 21.4
1RM Squat (kg)	108.9 ± 15.0	69.5 ± 18.7	89.2 ± 26.1
Enjoyment (PACES) — ABF	40.0 ± 7.8	40.0 ± 8.1	40.0 ± 7.9
Enjoyment (PACES) — GM	42.0 ± 8.3	43.0 ± 3.7	42.4 ± 6.4
<i>Physical activity level (IPAQ)</i>			
Low	2 (17%)	4 (33%)	6 (25%)
Moderate	1 (8%)	5 (42%)	6 (25%)
High	9 (75%)	3 (25%)	12 (50%)

Legend: Data are presented as mean ± standard deviation for continuous variables and n (%) for categorical variables. PACES-8 (range 8–56) was reported separately for ABF and GM. IPAQ follows the official short-form scoring protocol (Low/Moderate/High).

4.2.2 Instrumentation and Equipment

At the baseline session, anthropometric and body composition measurements were obtained using a TANITA BC-601 bioimpedance scale [68], a portable stadiometer, and a handheld digital dynamometer (OSDUE, model E108H, China) [69], the latter specifically for assessing maximal handgrip strength. In addition, participants completed an initial questionnaire with personal information, which also included the IPAQ [65] to assess their level of physical activity.

For the experimental sessions, several instruments and tools were employed to perform the exercises and to acquire biomechanical and physiological data. The exercises were

performed using the Speediance® GYM Monster 2 digital weight machine (Shanghai, China) [70]. The system offers a maximum load of 100 kg, adjustable in 0.5 kg increments, enabling the resistance to be adapted to each participant's needs for each exercise set.

To analyze the neuromuscular response to the two auditory stimuli during exercise, Acceleration (ACC), force, EMG, and Electrocardiography (ECG) signals were acquired. EMG measurements were recorded by placing two disposable Ag/AgCl adhesive electrodes per sensor cable, while three Ag/AgCl electrodes per cable were used for ECG. Acceleration was measured using a triaxial accelerometer, and force was recorded using a uniaxial load cell sensor. All sensors were connected to an eight-channel wireless Hub that transmitted data from each sensor to the *OpenSignals* software (version 2.2.5, PLUX Wireless Biosignals S.A., Lisbon, Portugal) [71]. These devices are all part of the *biosignalplux* Kit and all the sensors were provided by PLUX Biosignals S.A (Lisbon, Portugal) [71].

Additionally, a custom *Python* program was developed to establish a connection between the sensor channel of interest and the ABF tool. This software enabled Hub configuration, sensor selection, and real-time muscle signal sonification. To further control movement execution in the squat, the *My Jump Lab* App (version 5.0, Carlos Balsalobre, iOS/Android) [72] was used to check the execution angles and ensure, through verbal feedback, that all participants performed the movement within a similar range.

To allow auditory stimuli to be delivered without restricting movement and minimizing latency, participants used wired headphones connected to a computer via a 5-meter extension cable.

To perform the EMG real-time sonification, a sliding window was applied to smooth the signal's amplitude. The base sound was a 340 Hz sine wave, frequency-modulated by another 4 Hz sine wave. This low-frequency oscillator has its amplitude controlled by the EMG amplitude. The volume of the final sound is also controlled by the EMG amplitude. The samples were set to be stored in a 100 sample buffer. Rectification and smoothing of the signal's amplitude is done on a 0.1 s window. To normalize the signal an initial strong contraction was necessary as reference for the remaining data collection with live feedback.

At the end of each session, participants completed the PACES-8 [63] questionnaire to assess their subjective perception of enjoyment and satisfaction during the power test under the two auditory conditions.

4.2.3 Baseline Session

The session began with the reading and signing of the informed consent form. Afterwards, anthropometric and body composition measurements were collected, including body mass (kg), height (m), percentage of body fat, and percentage of fat-free mass. Maximal handgrip strength (kg) was also assessed, with each test repeated twice to ensure the maximum value was obtained.

To determine the loads to be applied during the power tests of the experimental sessions,

maximal strength (1RM) in the squat and bench press exercises was estimated using the coefficient method, an indirect estimation approach. In this procedure, participants performed as many repetitions as possible with a submaximal load, and the 1RM value was subsequently estimated by applying a tabulated coefficient. A detailed description of this method can be found in Appendix B.

4.2.4 Experimental Procedure

This section describes the experimental procedure of the study, including the setup of equipment and sensors, as well as the protocol followed during the experimental sessions.

4.2.4.1 Equipment and sensor setup

The triaxial accelerometer and load cell sensors were previously attached to the bar of the training machine. The accelerometer was placed under the load cell, aligning its z-axis with the direction of movement. The sensors were positioned to minimize mechanical noise resulting from the bar's movement during exercises.

For surface sensors, the skin areas of interest were prepared in advance by removing hair and cleaning with alcohol to optimize skin-electrode conductivity.

For EMG recordings, participants were instructed to contract the target muscles to facilitate anatomical identification. Electrodes were placed on the Triceps Brachii (at the midpoint between the posterior acromion and the olecranon) and on the Vastus Lateralis (VL) (at two-thirds of the line from the anterior superior iliac spine to the lateral border of the patella) of the dominant side, oriented parallel to the muscle fibers and over the muscle belly to ensure effective signal capture. The EMG reference electrode was placed over the olecranon process [73].

Subsequently, the three ECG electrodes were positioned to minimize motion artifacts, following a placement previously established by the researchers. The positive electrode was placed below the sternum, close to the medial plane and the negative electrode below the left breast, close to the nipple. The ground electrode was positioned on the manubrium, in the upper portion of the sternum.

All sensors were connected to the Hub and secured with an elastic band around the participant's waist to prevent interference with task performance. The signals were acquired at a sampling frequency of 1000 Hz and transmitted to the recording software.

Headphones were positioned and connected to the computer during the setup to ensure the delivery of auditory stimuli without interfering with task performance.

The setup of the sensors and equipment is illustrated in Figure 4.1.

4.2.4.2 Experimental Sessions

After setting up the equipment, resting signals were recorded for two minutes. This was followed by a standardized joint warm-up consisting of circular movements of the major

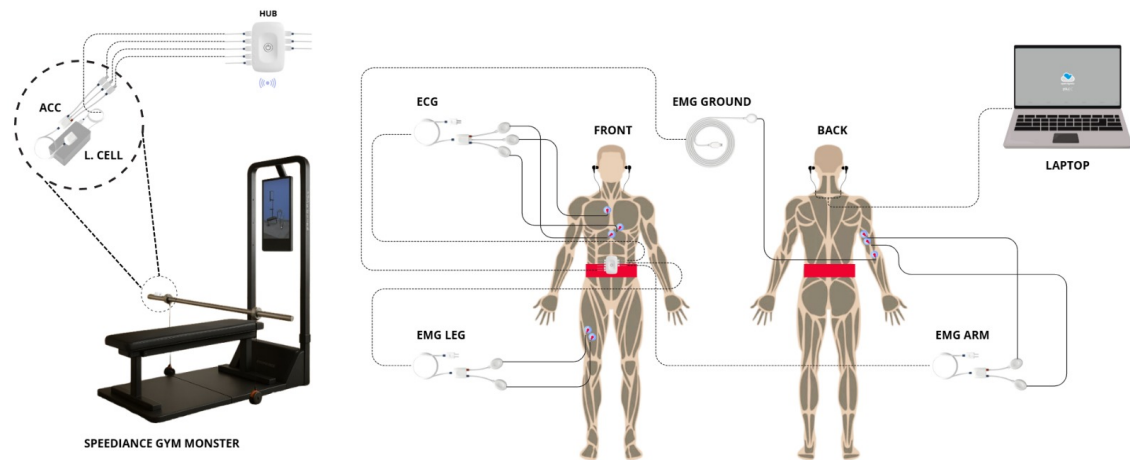


Figure 4.1: Equipment and sensor setup for signal acquisition.

segments for about five minutes. As part of the warm-up, since the power test exercises were performed in the order of bench press followed by squat, participants completed 10 repetitions with a moderate load before each exercise. The load was defined according to each subject's previous experience and individual capacity.

After the warm-up, participants began the power test. Test intensities were predetermined based on the 1RM values estimated during the baseline session. For the bench press, five sets were performed at relative loads of 30%, 40%, 50%, 60%, and 70% of 1RM; for the squat, five sets were performed at 40%, 50%, 60%, 70%, and 80% of 1RM. To minimize the risk of order or learning bias, the sequence of intensities and auditory conditions were randomized for each exercise.

For each exercise, subjects were exposed to two different auditory conditions: ABF and GM (predefined rhythmic music).

Randomization was applied independently for each exercise. This is, in the bench press, participants first completed five sets under one auditory stimulus (ABF or GM), and then repeated the sets under the other stimulus. For the squat, the order of the stimuli was randomized again and could differ from the bench press sequence.

Each intensity was performed in three consecutive repetitions, resulting in a total of 10 sets of 3 repetitions per exercise. The protocol included 2 minutes of rest between sets and 3 minutes of rest between exercises, following the recommendations of the American College of Sports Medicine (ACSM) [74], to minimize accumulated fatigue. The volunteers were instructed to perform all repetitions with a controlled eccentric phase, where movement speed and range of motion were verbally guided by the investigator, followed by a concentric phase at maximal intended velocity.

Recordings were performed under controlled laboratory conditions to maintain ambient temperature and humidity. Data acquisition was conducted in the Department of Physics (Laboratory 106) at the Faculdade de Ciências e Tecnologias da Universidade

Nova de Lisboa.

At the end of each session, participants performed simple stretches focusing on the main muscle groups involved, after which resting signals were collected for two minutes. Each participant completed three experimental sessions, all conducted under the same protocol and lasting approximately 90 minutes. The detailed experimental protocol is provided in Appendix C, while a schematic representation of a testing session is presented in Appendix D.

4.3 Signal Processing

For this study, only the ACC, load cell, and EMG data from the sensors were analyzed.

4.3.1 Units Conversion

The sensors provided raw digital values that needed to be converted into physical units. For this purpose, the transfer functions described in the technical data sheets for each sensor were applied [75], [76]. For the EMG sensor, each channel has a resolution of 16 bits ($n = 16$), with an operating voltage of $V_{CC} = 3 V$. The same voltage conditions were applied to the ACC sensor.

The loadcell physical values were obtained through static calibration using known reference masses. The resulting equation was:

$$F (N) = (a \cdot CH1 + b) \cdot g, \quad (4.1)$$

where $g = 9.81 \text{ m/s}^2$.

The transfer functions for the devices connected to the Hub are represented by the following equations:

$$EMG(V) = \frac{\left(\frac{ADC}{2^n} - \frac{1}{2}\right) \cdot V_{CC}}{G_{EMG}} \quad EMG(mV) = EMG(V) \cdot 1000 \quad (4.2)$$

where G_{EMG} is equal to 1009.

$$LOADCELL(N) = (-0.0029 \cdot ADC + 94.2825) \cdot 9.81 \quad (4.3)$$

For the ACC sensor, prior calibration was performed as instructed in the datasheet to obtain the C_{min} and C_{max} values corresponding to the calibration limits. The transfer equation is given by:

$$ACC(g) = \frac{ADC - C_{min}}{C_{max} - C_{min}} \times 2 - 1 \quad (4.4)$$

4.3.2 ACC Filtering

To reduce noise from the triaxial accelerometer, a third-order Butterworth bandpass filter (0.5–5 Hz) was applied to preserve the dynamic component of movement [77].

Then, the signal was further smoothed using a Gaussian filter [78]. The σ value used was 6 and determined experimentally to attenuate residual fluctuations without losing relevant information. The procedure was implemented using the *SciPy* library [79] and its `gaussian_filter1d` function. Finally, all accelerometer axes were converted from g-force to m/s^2 , $ACC_{m/s^2} = 9.8 \times ACC_g$. However, only the z-axis component (parallel to the vertical movement of the exercise) was used for the subsequent analyses and calculations.

4.3.3 Load Cell Filtering

To reduce the significant noise present in the load cell signal, a Gaussian filter with a σ value of 20 was applied [80]. A high sigma value was selected experimentally to provide stronger smoothing while preserving the overall signal trend, resulting in a more stable representation of the applied force.

4.3.4 Velocity Filtering

To obtain the velocity signal, the filtered acceleration data was integrated using the `cumulative_trapezoid` function from the *SciPy* [79] `integrate` module. This function applies the trapezoidal rule point by point to estimate the velocity at each instant by successively summing the areas under the acceleration curve while accounting for the sampling interval. The resulting velocity signal, expressed in m/s , was smoother and less noisy than the acceleration signal, making it more suitable for segmenting movement cycles.

The Seasonal-Trend decomposition using Loess (STL) method [81], implemented through the `statsmodels.tsa.seasonal` module, was applied to the integrated signal. A period of 300 samples was defined, as it provided the most effective balance between smoothing and signal preservation. Only the trend component of the decomposition was used, as it captured the underlying biomechanical pattern while removing high-frequency noise and irregular fluctuations present in the observed signal.

4.3.5 Power Filtering

Power was calculated as the point-to-point product of the raw velocity signal (m/s) and the filtered load cell signal (N). The resulting output corresponded to the instantaneous power signal, expressed in *Watt* (W). As with the velocity data, this signal was also smoothed using the STL method with the same parameters described above.

4.3.6 EMG Filtering

Before processing the EMG signal, the offset of the raw signal was removed. Then, a 4th-order Butterworth bandpass filter with cutoff frequencies between 10 Hz and 499 Hz was applied. This frequency range is commonly used to preserve the physiological content of surface EMG signals [82].

4.4 Algorithms

It should be noted that the detection and analysis procedures described in the following subsections were applied to each recorded file, under the same parameters and conditions. Each file therefore corresponds to a set of three repetitions.

4.4.1 Concentric Phase Detection Algorithm

The concentric phases of the movement were identified based on the positive peaks of the raw velocity signal. First, all local maxima of the velocity signal above a minimum threshold, defined by the variable *min_peak_height*, were detected. Then, the detected peaks were sorted by amplitude, and the *N* peaks (*num_peaks*) with the highest values were selected. To ensure that no more than one peak was assigned to each repetition, a minimum distance between peaks (*min_distance_s*) was imposed. For each detected peak, the beginning of the concentric phase was defined as the first zero-crossing immediately before the peak and the end of the concentric phase was defined as the first zero-crossing immediately after the peak. The algorithm parameters are specified in Table 4.2, and a schematic representation of the algorithm is provided in Appendix E .

Table 4.2: Parameters used in the Concentric Phase Detection Algorithm.

Variables	Assigned value	Description
<i>min_peak_height</i>	0.15 m/s	Minimum velocity threshold for a peak to be considered valid.
<i>num_peaks</i>	3	Number of peaks to detect (corresponding to the 3 repetitions per set).
<i>min_distance_s</i>	1.30 s	Minimum distance between consecutive peaks, ensuring that only one repetition is associated with each peak.

4.4.2 Repetition Start Detection Algorithm

The algorithm was developed based on the raw velocity signal and operates in two stages within a window, *window_back_s*, before each previously identified concentric start:

- i) It searches for the first zero-crossing (i.e, signal change) of the velocity whose distance to the concentric start is greater than or equal to *min_eccentric_duration*.
- ii) Once identified, the algorithm is refined by selecting the last local maximum immediately preceding the zero-crossing. This point is only considered if its velocity is less than or equal to *max_inflection_velocity* and if it occurs within *distance_to_zero_cross_sec* of the zero-crossing. This refinement was supported by

external validation: synchronization of resampled velocity signals with real-time motion video revealed that, in some cases, the actual start of the motion occurred slightly before the zero-crossing. If this maximum did not satisfy all conditions, the identified zero-crossing was considered the start of the repetition.

Each repetition ended exactly at the end of each concentric phase. The algorithm parameters are specified in Table 4.3, and a schematic representation of the algorithm is provided in Appendix E .

Table 4.3: Parameters used in the Repetition Start Detection Algorithm.

Variables	Assigned value	Description
window_back_s	1.70 s	Maximum backward search window before each concentric start.
min_eccentric_duration	0.60 s	Minimum required eccentric duration between the zero crossing (or inflection) and the concentric start.
max_inflection_velocity	0.03 m/s	Upper bound for the velocity at the inflection point to ensure a subtle deceleration close to zero.
distance_to_zero_cross_sec	0.01 s	Maximum allowed time gap between the inflection point and the zero crossing (proximity constraint).

4.4.3 EMG Onset Detection Algorithm

In order to identify the onset of concentric contraction for each repetition in the EMG signal, an EstOpt model-based algorithm was developed [83] . The original method is a statistical algorithm that models the onset as a decision problem between two probabilistic regimes: before the onset, the signal is basal noise, and after the onset, the signal is described as a rising ramp. The estimate is obtained through maximum likelihood, seeking the optimal instant that minimizes the quadratic error of each model.

The algorithm developed can be considered as a simplified and deterministic version of the existing model and can be described by the following sequential steps:

1. Application of the Teager-Kaiser Energy Operator (TKEO): This operator estimates the signal's instantaneous energy, which is consistent with muscle activation. This results in greater sensitivity to abrupt transitions, highlighting the onset, while reducing slow variations in the signal that can mask the actual start of the movement.
2. Rectification and Gaussian smoothing: Passage to absolute value and application of a Gaussian filter over time ($\sigma = 50$ ms). The resulting signal is a continuous and stable envelope of muscle energy.

3. Onset detection criterion: For each analysis window preceding the start of each concentric phase, $window_ms$, a candidate onset k is evaluated. Before k , it is assumed that the envelope is modeled by a constant baseline level ($E_{pre}(t) = \sum_{n=0}^t (e(n) - \bar{e}_{pre})^2$), whereas after k , it is modeled by a linear regression representing the envelope rise ($E_{post}(t) = \sum_{n=t}^N (e(n) - \hat{e}_{lin}(n))^2$). The EMG onset is defined as the point k that minimizes the sum of the quadratic errors of the two models ($t_0 = 2 \min_t (E_{pre}(t) + E_{post}(t))$).

Additionally, the variables *guard* and *min_window* were also defined to (i) avoid false onsets at the edges of the window and (ii) ensure that the window contained enough signal to distinguish basal noise from muscle activation. The algorithm parameters are specified in Table 4.4, and steps 1–3 are illustrated in Appendix E.

Table 4.4: Parameters used in the EMG Onset Detection Algorithms.

Variables	Assigned value	Description
sigma_ms	50 ms	Standard deviation of the Gaussian kernel used to smooth the TKEO-based envelope.
window_ms	300 ms	Backward analysis window before each concentric start in which the EMG onset is searched.
guard	10 ms	Exclusion margin at the window edges to avoid spurious detections near boundaries.
min_window	100 ms	Minimum usable window length to ensure sufficient signal for reliable onset estimation.

Legend: TKEO – Teager–Kaiser Energy Operator.

4.5 Metrics

To ensure the metrics applied only to the relevant segments of the movement (three repetitions and their respective concentric phases), the signals were cut. Each signal was segmented two seconds before the start of the first repetition and three seconds after the end of the last repetition.

4.5.1 Maximum Velocity

The Maximum Velocity value in each repetition, expressed in m/s , was obtained in two steps:

- i) For each segment corresponding to the beginning and the end of each concentric phase, the index of the maximum peak in the filtered velocity signal was identified to ensure greater robustness and lower sensitivity to noise.
- ii) For the same segment, the value at the identified index was extracted from the raw velocity signal to preserve the actual magnitude of the signal.

4.5.2 Maximum Power

The Maximum Power value, expressed in *Watt (W)*, was calculated using the same procedure already explained above for Maximum Velocity. For each concentric phase, the time instant of the peak power in the filtered signal was detected, and the corresponding value at that instant was extracted from the raw signal. Since measurements were taken only from the dominant hand's side, the obtained values corresponded only to unilateral power. Therefore, a scaling factor of 2 was applied, assuming anatomical symmetry between limbs.

4.5.3 Velocity Power Difference

For each repetition, the time difference between the instant of the maximum peak in the filtered velocity signal and the instant of the maximum peak in the filtered power signal was calculated. The result was expressed in *seconds (s)*.

4.5.4 Correlation of Repetition Profiles

The correlation among the temporal profiles of each repetition was quantified by evaluating the consistency of the velocity and acceleration curve patterns. This analysis was performed only on these signals because they directly represent the kinematic pattern of the movement. First, each concentric phase was normalized through linear interpolation so that all curves contained 100 points, representing 0–100% of the concentric phase. A Pearson correlation matrix was then constructed from these normalized segments to assess the linear similarity of the profile shapes over the normalized time. Finally, unique pairs of correlation values were extracted from the matrix, corresponding to the comparison of each possible pair of repetitions.

4.5.5 Peak Velocity and Peak Power Index

To extract relevant information on neuromuscular coordination and force application efficiency, a temporal analysis was performed on the instants when peak velocity and peak power occurred in each repetition. First, each concentric phase was time-normalized as described in subsection 4.5.4. Then, the index corresponding to the maximum value of each signal within each concentric phase was identified and converted into the relative percentage of the concentric cycle at which it occurred. This approach made it easier to compare peaks both across repetitions and between signals over time.

4.5.6 Peak Rate of Power Development

In order to characterize the speed at which the power signal increased throughout the concentric phase, the Rate of Power Development (RPD) defined as the temporal derivative of power ($\frac{dP}{dt}$), was calculated using the gradient function from the NumPy module. This process was applied to the filtered power signal in order to reduce the noise amplification associated with differentiation. For each repetition, the maximum derivative value, expressed in W/s , and the respective instant were obtained. Higher values indicate a faster rise in power, reflecting more effective neuromuscular coordination at the onset of the concentric phase.

4.5.7 Window and Total Power Slopes

To characterize the temporal evolution of power from the beginning of the concentric phase to the maximum peak power of each repetition, the slope of the signal was calculated. This approach consisted of two aspects:

1. Segmental slopes: The defined segment was divided into consecutive windows with a fixed duration of 50 *ms*. The slope was then calculated as the variation in power per unit of time within each window, expressed in W/s . This division provided a more detailed and instantaneous evolution of power development.
2. Total slope: The slope was also calculated as the ratio between the difference in power values at the boundaries of the segment and the corresponding time interval, expressed in W/s . This measure reflected the average rate of power increase across the entire concentric effort.

4.5.8 EMG Onset to Peak Power

To assess the temporal effectiveness of how electrical muscle activation translates into the expression of peak power, the time delay, expressed in *seconds* (*s*), between EMG onset and the maximum peak power during the concentric phase was measured.

4.5.9 EMG Rise Time and Slope

In order to quantify the temporal efficiency of EMG activation up to its maximum peak, the time delay, in *seconds*, between the EMG onset (the start of electrical activation) and the envelope peak (maximum electrical activation) was calculated. The peak was defined as the maximum local value of the Gaussian envelope (described in Subsection 4.4.3) that occurs after the estimated onset and, when specified, within a bounded search window after it (0.5 *s*). To improve robustness, only peaks showing a decline over the next 60 *ms* were accepted; this was verified by requiring a negative average sample-to-sample change in that window. When needed, a minimum peak prominence threshold was also applied to suppress spurious fluctuations.

Based on the same envelope peak, and in order to quantify how quickly the electrical activity rose from the EMG onset to the peak, the slope was calculated as the ratio between the change in envelope amplitude and the corresponding time interval. The value was expressed in mV/s .

4.5.10 EMG Median Frequency

The EMG median frequency corresponds to the frequency that divides the power spectrum into two regions of equal power. In this study, the median frequency of the filtered EMG signal was calculated from the EMG onset to the end of each repetition. The calculation consisted of the following steps:

1. Spectral power density estimation: The power spectral density was computed using the *Welch* method, with windows of maximum length $\text{sampling frequency/seconds}$ samples (or the segment length if shorter), providing a balance between spectral resolution and stability.
2. Cumulative integration: The spectral density was then integrated cumulatively in order to calculate the accumulated power as a function of frequency (total power).
3. Median frequency determination: The median frequency was identified as the frequency below which 50% of the total spectral power is concentrated, indicating the energy distribution of the EMG spectrum.

This metric is widely used to assess muscle fatigue and to observe changes in motor unit recruitment.

4.6 Data Organization and Database Structure

All raw data were processed and organized into a hierarchical folder structure based on participant, session and auditory stimulus. Each participant's folder contains subfolders for each session, and each session is divided into two folders corresponding to the auditory stimuli (ABF and GM). Within each stimulus folder, the text files with the raw data are stored in the *Files* directory, while the output images generated during processing are saved in the *Plots* directory. The *Plots* directory is further subdivided by exercise type (bench press or squat). A simplified diagram of the data structure and storage is presented in Figure 4.2.

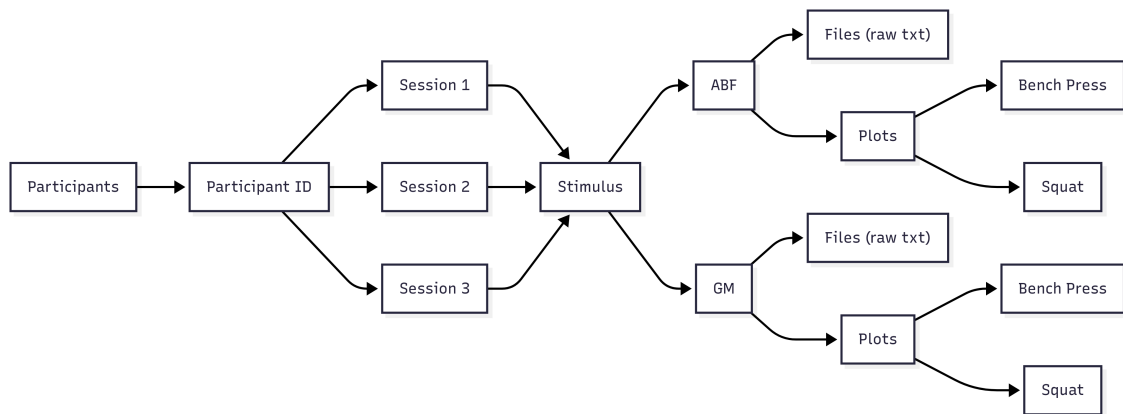


Figure 4.2: Directory structure for participant data storage.

At the same time, a nested dictionary, *participants_data*, was created to store the processed information in memory. This dictionary reproduces the same structure as the database: the keys follow the hierarchy from participant to session, then to stimulus and exercise, and the final values correspond to lists of text files representing the repetitions of a given set.

Batch processing was implemented using a function that iteratively ran through all participants, sessions, and stimuli, automatically calling the signal processing pipeline for each file. Extracted metrics were stored in a structured dictionary, *results_per_participant*, with metadata along with the results for each file and each repetition. The processed data were exported to CSV format for statistical analysis. Outliers were then identified using the z-score method and excluded when exceeding three standard deviations from the mean.

4.7 Statistical Analysis

All statistical analyses were performed in JASP (Version 0.95; JASP Team, University of Amsterdam) [84], where the Bayesian repeated-measures ANOVA is implemented as a mixed-effects model including participants as random effects, with random slopes specified for repeated measures factors. Numerical accuracy was set to manual with 10000 samples and a fixed random seed to ensure stability and reproducibility of Bayes Factor estimates. For each exercise and session, only the signals corresponding to the load at which each participant achieved their highest power output were retained for statistical analysis, under both auditory conditions.

4.7.1 Full-Sample Analysis

A Bayesian two-way repeated-measures ANOVA was employed to analyze the data. To test whether the dependent variables varied across sessions and stimuli, a factorial design with two within-subject factors (Session and Stimulus) was applied to the full dataset. The

analyses were conducted separately for the bench press and squat exercises and applied to each dependent variable of interest. The Bayesian framework was selected given the cross-sectional design of this study. This approach is particularly advantageous under small-sample conditions and in exploratory contexts [85], as it avoids reducing inference to dichotomous “significant” versus “non-significant” decisions [86]. Instead, Bayes Factors provide a continuous measure of the strength of evidence, enabling a more nuanced interpretation of whether ABF influenced performance outcomes. The classification of evidence strength followed Jeffreys’ conventional scale [87], where values of Bayes Factor between 1 and 3 are considered anecdotal, between 3 and 10 moderate, and above 10 strong to decisive.

It should be noted that, for each table presented in the following chapter, only the best-fitting model is reported. The best model is defined as the one with the highest posterior model probability $P(M | \text{data})$, which quantifies the relative likelihood of a model given the observed data [87]. Post-hoc comparisons were performed only for metrics where Session contributed to model fit, given its three levels. Results are expressed as Bayes Factor ($BF_{10,U}$), together with the associated error percentage.

In addition, Gender was included as a between-subject factor to account for potential differences between male and female participants, and body mass was added as a covariate to examine whether the effects of Session and Stimulus were consistent across sexes after controlling for body mass.

4.7.2 Sex-Specific Analysis

The data were stratified by sex, and separate Bayesian two-way repeated-measures ANOVAs were carried out for male and female participants within each exercise. In each stratified analysis, participants’ physical activity level, as assessed by the IPAQ questionnaire, was included as a covariate to examine its potential impact on the dependent variables. All conventions described above regarding evidence classification, reporting of the best-fitting model, and the use of post-hoc comparisons were likewise applied to these sex-stratified analyses.

Complementary tables from both the overall and the sex-specific analyses, including all other candidate models tested for the metrics that showed evidence for the inclusion of the factor Session in the best model, are provided in Appendix F.

4.7.2.1 Quantifying Adaptation

From the sex-stratified analyses, the dependent variables with the strongest evidence of systematic effects were identified. In most of these variables, Session consistently appeared as one of the key factors, highlighting the progressive evolution across sessions. To further quantify these changes across stimuli, pairwise comparisons were carried out between Session 1 and Session 2 and between Session 1 and Session 3. Bayesian paired-samples t-tests were then performed separately by sex, stimulus condition, and exercise. The

alternative hypothesis specified that performance in the later session would exceed that in the earlier one (Measure 1 < Measure 2). Prior to these analyses, the normality of the difference scores was verified using the Shapiro–Wilk test, which confirmed compatibility with a normal distribution. On this basis, Student’s t was adopted as the statistical test, and evidence was expressed using the Bayes Factor (BF_{-0}).

4.7.2.2 Perceived Enjoyment

Finally, participants’ perceived enjoyment during the power test with ABF and GM was evaluated using a Bayesian repeated-measures ANOVA, with Session and Stimulus as within-subject factors and Gender as a between-subject factor.

RESULTS

This chapter presents the results of this thesis research, structured into two analyses of the metrics proposed in Chapter 4. The first analysis includes all participants, with results reported separately for each exercise. The second provides a sex-specific analysis, where results are also presented by exercise.

5.1 Overall Analysis Across Participants

The results from the Bayesian two-way repeated-measures ANOVA for all metrics are presented in Table 5.1 for the bench press and in Table 5.2 for the squat. Although Gender was included as a between-subject factor in the analyses, only the overall descriptive statistics are reported, without stratification by sex.

Table 5.1: Bayesian repeated-measures ANOVA results for all evaluated metrics in the bench press exercise.

Variables	Session						BestM	P(M data)	BF_M	R^2
	S1		S2		S3					
	ABF	GM	ABF	GM	ABF	GM				
Max Power (W)	146.7 ± 95.4	146.7 ± 97.8	151.6 ± 102.5	152.0 ± 101.6	166.9 ± 120.5	161.0 ± 116.0	S+G+S*G	0.323	17.686	0.941
Max Velocity (m/s^2)	0.8 ± 0.3	0.8 ± 0.3	0.8 ± 0.3	0.7 ± 0.3	0.9 ± 0.3	0.8 ± 0.3	S+G+BM+S*G	0.138	5.911	0.692
Peak RPD (W/s)	250.3 ± 156.3	249.4 ± 156.6	252.5 ± 150.0	268.2 ± 167.7	268.0 ± 171.4	275.6 ± 192.9	S+G+S*G	0.115	4.820	0.907
PP Index (%)	46.5 ± 4.1	48.3 ± 6.8	47.7 ± 6.1	47.2 ± 3.8	46.8 ± 4.2	47.0 ± 4.7	NM	0.223	10.629	0.435
PV Index (%)	52.2 ± 3.5	54.0 ± 5.4	53.3 ± 5.1	52.7 ± 3.5	52.3 ± 3.4	52.4 ± 4.3	NM	0.198	9.152	0.427
Velocity Power Dif (ms)	25.0 ± 12.0	25.0 ± 14.0	24.0 ± 11.0	24.0 ± 10.0	23.0 ± 11.0	23.0 ± 10.0	G	0.292	15.241	0.594
TP Slope (W/s)	169.5 ± 100.2	168.4 ± 99.5	167.3 ± 93.7	184.6 ± 111.0	177.9 ± 106.2	186.9 ± 128.3	G	0.155	6.807	0.873
WP Slope (W/s)	187.3 ± 112.2	185.9 ± 109.4	183.1 ± 102.6	206.7 ± 127.5	201.0 ± 122.8	211.9 ± 146.5	G	0.086	3.483	0.865
Velocity Corr (-)	1.0 ± 0.1	1.0 ± 0.0	1.0 ± 0.1	1.0 ± 0.0	1.0 ± 0.0	1.0 ± 0.0	NM	0.228	10.944	0.409
ACC Corr (-)	1.0 ± 0.1	1.0 ± 0.1	1.0 ± 0.1	1.0 ± 0.1	1.0 ± 0.0	1.0 ± 0.0	NM	0.157	6.884	0.510
EMG Rise Time (s)	0.5 ± 0.2	0.5 ± 0.2	0.5 ± 0.2	0.5 ± 0.2	0.4 ± 0.1	0.5 ± 0.2	S+G+BM+S*G	0.154	6.712	0.721
EMG Rise Slope (mV/s)	0.1 ± 0.1	0.1 ± 0.1	0.1 ± 0.1	0.1 ± 0.1	0.1 ± 0.2	0.1 ± 0.2	G	0.174	7.791	0.673
EMG Onset to PP (s)	0.3 ± 0.1	0.4 ± 0.1	0.3 ± 0.1	0.3 ± 0.1	0.3 ± 0.0	0.3 ± 0.1	BM	0.225	10.721	0.514
EMG Median Freq (Hz)	65.5 ± 9.3	65.1 ± 10.7	63.9 ± 10.2	64.2 ± 9.1	63.4 ± 9.8	63.5 ± 10.6	NM	0.392	11.604	0.713

Legend: Max- Maximum; RPD- Rate of Power Development; PP- Peak Power; PV- Peak velocity; Dif- Difference; TP- Total Power; WP- Window Power; Corr- Correlation; ACC- Acceleration; Freq- Frequency; BestM- Best Model; S- Session; G- Gender; BM- Body Mass; NM- Null Model; P(M | data)- posterior model probability; BF_M - Bayes Factor comparing the best model to all others; R^2 - explained variance of the model; "+" indicates inclusion of main effects; "*" indicates inclusion of the interaction between factors. Results in bold reflect greater evidence with Session included.

The following analysis refers to the bench press exercise.

Regarding Maximum Power, the best model received very strong support ($BF_M = 17.686$), highlighting Session effects and sex differences as the main determinants of this metric. A near-equivalent model additionally including body mass ($BF_M = 15.060$) suggested only a minor contribution of the covariate. Post-hoc comparisons for sessions showed moderate evidence for Session 2 and Session 3 (S2-S3) ($BF_{10,U} = 3.818$, $\epsilon < 0.001$) and strong evidence for S1-S3 ($BF_{10,U} = 7.698$, $\epsilon < 0.001$).

Concerning Peak RPD, evidence was moderate ($BF_M = 4.820$) for the best model, with Gender alone also being highly explanatory ($BF_M = 4.374$). Post-hoc session contrasts provided at most anecdotal evidence, consistent with the relatively low model probability ($P(M | \text{data}) = 0.115$) and fragmented support across models.

With respect to Maximum Velocity, the best model showed moderate support ($BF_M = 5.911$), nearly identical to the model without body mass ($BF_M = 5.826$). Post-hoc tests indicated moderate-to-strong evidence for session effects, particularly S1-S3 ($BF_{10,U} = 7.606$, $\epsilon < 0.001$) and S2-S3 ($BF_{10,U} = 3.213$, $\epsilon < 0.001$).

As for EMG Rise Time, the best model showed moderate-to-strong support ($BF_M = 6.712$), while a nearly equivalent model with the same factors but without body mass yielded a similar level of evidence ($BF_M = 6.425$). Post-hoc tests revealed moderate evidence for differences in S1-S3 ($BF_{10,U} = 4.932$, $\epsilon < 0.001$). In Figure 5.1, the increasing evolution of these variables across sessions by sex is shown for the bench press exercise.

The variability of Velocity Power Difference, Total Power Slope, Window Power Slope, and EMG Rise Slope was primarily explained by sex differences ($BF_M \in [3.482, 15.241]$). For EMG Onset to Peak Power, body mass emerged as the dominant predictor ($BF_M = 10.721$). The remaining metrics are not explained by any of the independent factors, with the null model receiving the strongest support.

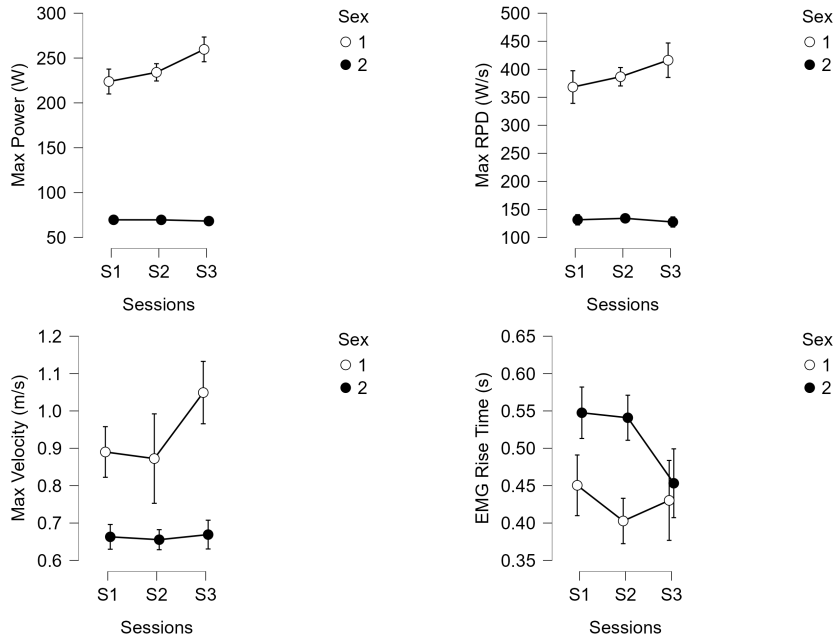


Figure 5.1: Descriptive plots of the variables most influenced by Session and Gender, highlighting their progressive evolution across sessions in the bench press exercise. S = Session; 1 = Male, 2 = Female.

Table 5.2: Bayesian repeated-measures ANOVA results for all evaluated metrics in the squat exercise.

Variables	Session						BestM	P(M data)	BF _M	R ²
	S1		S2		S3					
	ABF	GM	ABF	GM	ABF	GM				
Max Power (W)	298.6 ± 126.3	302.1 ± 121.4	328.8 ± 148.5	334.4 ± 146.5	330.1 ± 145.5	344.0 ± 164.8	S+G+BM + S*G	0.336	18.720	0.885
Max Velocity (m/s ²)	0.5 ± 0.1	0.5 ± 0.2	0.5 ± 0.1	0.5 ± 0.1	0.5 ± 0.2	0.5 ± 0.2	G	0.123	5.175	0.709
Peak RPD (W/s)	450.9 ± 177.6	466.0 ± 194.2	498.7 ± 234.9	498.9 ± 220.0	492.7 ± 237.4	519.5 ± 257.5	S+G+BM + S*G	0.245	11.987	0.859
PP Index(%)	69.1 ± 7.4	67.4 ± 8.3	70.7 ± 8.5	71.5 ± 9.0	71.2 ± 8.7	69.7 ± 7.1	S+G	0.113	4.737	0.623
PV Index (%)	69.6 ± 7.0	68.3 ± 7.7	71.2 ± 8.0	71.9 ± 8.5	71.8 ± 8.2	70.1 ± 6.8	G	0.116	4.865	0.626
Velocity Power Dif (ms)	3.0 ± 3.0	5.0 ± 5.0	3.0 ± 4.0	3.0 ± 4.0	3.0 ± 3.0	3.0 ± 3.0	NM	0.163	7.188	0.487
TP Slope (W/s)	249.2 ± 123.0	272.1 ± 152.7	271.1 ± 199.7	262.8 ± 189.7	265.9 ± 209.8	284.8 ± 203.8	G+BM	0.242	11.837	0.756
WP Slope (W/s)	261.1 ± 129.4	288.1 ± 164.5	285.9 ± 215.1	278.5 ± 209.2	282.6 ± 230.6	298.6 ± 217.7	G+BM	0.210	9.836	0.804
Velocity Corr (-)	0.9 ± 0.2	0.8 ± 0.2	0.8 ± 0.2	0.9 ± 0.1	0.8 ± 0.2	0.8 ± 0.2	NM	0.354	20.310	0.352
ACC Corr (-)	0.9 ± 0.1	0.9 ± 0.1	0.9 ± 0.1	0.9 ± 0.1	0.9 ± 0.1	0.9 ± 0.1	NM	0.293	15.355	0.218
EMG Rise Time (s)	0.4 ± 0.2	0.4 ± 0.2	0.4 ± 0.2	0.5 ± 0.2	0.4 ± 0.1	0.5 ± 0.2	NM	0.237	11.488	0.374
EMG Rise Slope (mV/s)	0.1 ± 0.1	0.1 ± 0.1	0.1 ± 0.1	0.1 ± 0.1	0.1 ± 0.1	0.1 ± 0.1	BM	0.157	6.881	0.439
EMG Onset to PP (s)	0.7 ± 0.1	0.7 ± 0.3	0.7 ± 0.2	0.7 ± 0.2	0.7 ± 0.3	0.7 ± 0.2	NM	0.191	8.753	0.628
EMG Median Freq (Hz)	64.0 ± 7.5	65.9 ± 8.2	68.2 ± 9.5	67.1 ± 12.6	63.9 ± 9.3	65.1 ± 7.4	NM	0.149	6.464	0.465

Legend: Max- Maximum; RPD- Rate of Power Development; PP- Peak Power; PV- Peak Velocity; Dif- Difference; TP- Total Power; WP- Window Power; Corr- Correlation; ACC- Acceleration; Freq- Frequency; BestM- Best Model; S- Session; G- Gender; BM- Body Mass; NM- Null Model; P(M | data)- posterior model probability; BF_M- Bayes Factor comparing the best model to all others; R²- explained variance of the model; “+” indicates inclusion of main effects; “*” indicates inclusion of the interaction between factors. Results in bold reflect greater evidence with Session included.

Regarding the squat, certain effects were consistent with those observed in the bench press.

There was very strong evidence ($BF_M = 18.720$) that Session, Gender, and their interaction were the key determinants of the variable Maximum Power, with body mass further strengthening the model. A nearly equivalent model without this covariate (BF_M

= 11.511) confirmed that the main effects were driven by Session and Gender. The post-hoc tests were consistent with this pattern, with strong to very strong evidence for session differences (S1–S2: $BF_{10,U} = 22.629$, $\epsilon < 0.001$; S1–S3: $BF_{10,U} = 55.980$, $\epsilon < 0.001$).

Peak RPD followed a similar profile: the best model had strong support ($BF_M = 11.987$), while the version without body mass remained strongly supported ($BF_M = 7.277$), implying a relevant but secondary contribution of this covariate. The post-hoc results showed moderate session effects (S1–S2: $BF_{10,U} = 5.879$, $\epsilon < 0.001$; S1–S3: $BF_{10,U} = 6.038$, $\epsilon < 0.001$). Figure 5.2 illustrates the upward progression of these variables across sessions for each sex in the squat exercise.

For Peak Power Index, although the evidence was somewhat fragmented, the most probable model was supported by moderate evidence ($BF_M = 4.737$), with a nearly equivalent model including Gender alone ($BF_M = 4.364$). This indicates that sex was the primary explanatory factor. Post-hoc tests were consistent with this finding, showing moderate evidence for session differences (S1–S2: $BF_{10} = 4.128$, $\epsilon < 0.001$).

Despite the fragmented nature of the evidence, the variability of Maximum Velocity and Peak Velocity Index was mainly explained by sex differences ($BF_M = 5.175$ and $BF_M = 4.865$, respectively). For Total Power Slope and Window Power Slope, there was also strong evidence that Gender was the dominant factor, with body mass adding only a marginal contribution ($BF_M = 9.611$ and $BF_M = 9.836$, respectively). EMG Rise Slope was primarily predicted by body mass ($BF_M = 6.881$), followed by Gender, which also showed relevance on its own ($BF_M = 6.483$).

In contrast, none of the tested factors substantially explained the variance of the other metrics, with the null model receiving the strongest support.

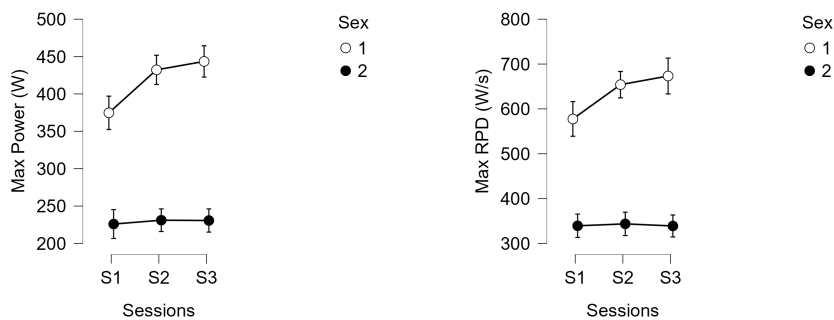


Figure 5.2: Descriptive plots of the variables most influenced by Session and Gender, highlighting their progressive evolution across sessions in the squat exercise. S = Session; 1 = Male, 2 = Female.

5.2 Sex-Specific Analysis

In this section, a detailed analysis by sex is presented.

5.2.1 Male Participants Analysis

The results from the Bayesian two-way repeated-measures ANOVA for all metrics are presented in Table 5.3 in the bench press.

Table 5.3: Bayesian repeated-measures ANOVA results for all evaluated metrics in the bench press exercise among male participants.

Variables	Session						BestM	P(M data)	BF_M	R^2
	S1		S2		S3					
	ABF	GM	ABF	GM	ABF	GM				
Max Power (W)	223.8 ± 72.7	223.8 ± 78.9	232.7 ± 81.4	235.4 ± 74.7	265.2 ± 92.7	254.1 ± 91.3	S	0.319	4.217	0.884
Max Velocity (m/s^2)	0.9 ± 0.3	0.9 ± 0.3	0.9 ± 0.3	0.8 ± 0.3	1.1 ± 0.3	1.0 ± 0.3	S	0.273	3.381	0.537
Peak RPD (W/s)	371.6 ± 129.6	364.9 ± 134.7	371.0 ± 116.5	402.3 ± 130.5	406.9 ± 130.4	425.3 ± 163.1	S	0.162	1.745	0.643
PP Index (%)	47.6 ± 4.3	49.0 ± 7.7	49.4 ± 7.6	47.7 ± 2.9	47.6 ± 2.7	48.0 ± 2.9	NM	0.362	5.108	0.416
PV Index (%)	51.9 ± 3.1	53.0 ± 6.6	53.8 ± 6.0	52.3 ± 2.8	52.1 ± 1.1	52.6 ± 2.3	NM	0.359	5.047	0.409
Velocity Power Dif (ms)	17.0 ± 7.0	16.0 ± 7.0	17.0 ± 7.0	18.0 ± 5.0	17.0 ± 6.0	18.0 ± 5.0	NM	0.365	5.176	0.328
TP Slope (W/s)	245.4 ± 84.8	240.4 ± 84.7	239.0 ± 75.1	273.1 ± 85.2	263.1 ± 80.0	283.4 ± 113.9	PAL	0.196	2.190	0.637
WP Slope (W/s)	270.9 ± 96.6	266.6 ± 91.5	260.5 ± 82.8	308.4 ± 97.8	299.5 ± 92.6	322.2 ± 129.1	S+PAL	0.141	1.479	0.620
Velocity Corr (-)	1.0 ± 0.1	1.0 ± 0.0	1.0 ± 0.0	1.0 ± 0.0	1.0 ± 0.0	1.0 ± 0.0	NM	0.316	4.155	0.242
ACC Corr (-)	0.9 ± 0.1	1.0 ± 0.1	1.0 ± 0.1	1.0 ± 0.1	1.0 ± 0.0	1.0 ± 0.0	NM	0.294	3.745	0.276
EMG Rise Time (s)	0.5 ± 0.2	0.4 ± 0.2	0.4 ± 0.1	0.4 ± 0.1	0.4 ± 0.1	0.5 ± 0.2	NM	0.253	3.041	0.618
EMG Rise Slope (mV/s)	0.2 ± 0.1	0.2 ± 0.2	0.1 ± 0.1	0.2 ± 0.1	0.2 ± 0.2	0.2 ± 0.2	NM	0.242	2.866	0.703
EMG Onset to PP (s)	0.3 ± 0.1	0.3 ± 0.1	0.3 ± 0.1	0.3 ± 0.1	0.3 ± 0.0	0.3 ± 0.1	NM	0.335	4.529	0.434
EMG Median Freq (Hz)	63.5 ± 7.7	64.0 ± 10.1	62.7 ± 9.4	62.8 ± 6.3	63.1 ± 8.2	60.8 ± 9.1	NM	0.399	5.971	0.481

Legend: Max- Maximum; RPD- Rate of Power Development; PP- Peak Power; PV- Peak Velocity; Dif- Difference; TP- Total Power; WP- Window Power; Corr- Correlation; ACC- Acceleration; Freq- Frequency; BestM - Best Model; S- Session; PAL- Physical Activity Level; NM- Null Model; P(M | data)- posterior model probability; BF_M - Bayes Factor comparing the best model to all others; R^2 - explained variance of the model; "+" indicates inclusion of main effects. Results in bold reflect greater evidence with Session included.

For Maximum Power, Session was the strongest determinant ($BF_M = 4.217$), with moderate support. The next most probable model included physical activity level ($BF_M = 3.173$), suggesting only a limited additional contribution. Post-hoc tests indicated the largest differences between S1–S3 ($BF_{10,U} = 22.550$, $\epsilon < 0.001$) and S2–S3 ($BF_{10,U} = 23.310$, $\epsilon < 0.001$).

For Maximum Velocity, the best model also included Session alone, with moderate evidence ($BF_M = 3.381$), supported by strong differences between S1–S3 ($BF_{10,U} = 17.397$, $\epsilon < 0.001$) and moderate evidence for S2–S3 ($BF_{10,U} = 3.563$, $\epsilon < 0.001$). In contrast, Peak RPD was best explained by Session, but with only anecdotal evidence, indicating that no single factor clearly accounted for this metric.

For Total Power Slope and Window Power Slope, physical activity level consistently appeared among the best predictors, although without strong statistical support. By comparison, the null model was favored the remaining power- and velocity-related metrics, showing that none of the tested factors substantially explained their variance.

For all EMG-derived metrics, model comparisons also consistently favored the null model.

The results from the Bayesian two-way repeated-measures ANOVA for all metrics are presented in Table 5.4 in the squat.

Table 5.4: Bayesian repeated-measures ANOVA results for all evaluated metrics in the squat exercise among male participants.

Variables	Session						BestM	P(M data)	BF_M	R^2
	S1		S2		S3					
	ABF	GM	ABF	GM	ABF	GM				
Max Power (W)	378.8 ± 109.2	370.7 ± 110.2	429.0 ± 132.1	435.5 ± 125.1	434.5 ± 121.6	452.5 ± 149.4	S	0.380	5.525	0.729
Max Velocity (m/s^2)	0.5 ± 0.1	0.6 ± 0.2	0.6 ± 0.2	0.6 ± 0.2	0.6 ± 0.2	0.6 ± 0.2	NM	0.267	3.283	0.660
Peak RPD (W/s)	572.7 ± 124.9	582.5 ± 161.7	659.6 ± 199.1	648.4 ± 174.7	661.5 ± 201.2	685.1 ± 236.0	S	0.364	5.144	0.835
PP Index (%)	67.8 ± 8.1	64.5 ± 8.2	68.4 ± 9.0	68.1 ± 10.3	68.4 ± 10.0	67.4 ± 5.9	NM	0.336	4.554	0.561
PV Index (%)	68.3 ± 7.8	65.4 ± 7.8	68.9 ± 8.6	68.7 ± 9.6	69.0 ± 9.4	67.7 ± 5.7	NM	0.335	4.537	0.564
Velocity Power Dif (ms)	3.0 ± 2.0	4.0 ± 3.0	3.0 ± 3.0	3.0 ± 4.0	3.0 ± 4.0	3.0 ± 2.0	NM	0.365	5.170	0.417
TP Slope (W/s)	335.7 ± 109.5	372.5 ± 150.9	396.4 ± 212.9	383.0 ± 197.5	392.0 ± 234.3	398.9 ± 212.7	NM	0.270	3.332	0.662
WP Slope (W/s)	352.4 ± 113.6	395.5 ± 162.6	419.8 ± 230.7	409.8 ± 220.5	420.3 ± 258.7	419.7 ± 228.3	NM	0.272	3.364	0.775
Velocity Corr (-)	0.8 ± 0.2	0.8 ± 0.2	0.9 ± 0.1	0.9 ± 0.2	0.9 ± 0.1	0.8 ± 0.3	NM	0.359	5.049	0.472
ACC Corr (-)	0.9 ± 0.1	0.9 ± 0.2	1.0 ± 0.1	0.9 ± 0.1	1.0 ± 0.0	0.9 ± 0.1	NM	0.203	2.290	0.258
EMG Rise Time (s)	0.4 ± 0.2	0.4 ± 0.1	0.4 ± 0.2	0.5 ± 0.2	0.4 ± 0.2	0.5 ± 0.1	NM	0.323	4.302	0.417
EMG Rise Slope (mV/s)	0.1 ± 0.1	0.1 ± 0.1	0.1 ± 0.1	0.1 ± 0.1	0.2 ± 0.2	0.1 ± 0.1	PAL	0.351	4.876	0.211
EMG Onset to PP (s)	0.6 ± 0.1	0.7 ± 0.4	0.7 ± 0.2	0.7 ± 0.2	0.6 ± 0.2	0.6 ± 0.1	NM	0.390	5.759	0.586
EMG Median Freq (Hz)	64.2 ± 7.8	63.6 ± 7.3	66.7 ± 8.5	64.9 ± 11.0	61.9 ± 9.0	63.2 ± 5.0	NM	0.230	2.681	0.544

Legend: Max- Maximum; RPD- Rate of Power Development; PP- Peak Power; PV- Peak Velocity; Dif- Difference; TP- Total Power; WP- Window Power; Corr- Correlation; ACC- Acceleration; Freq- Frequency; BestM- Best Model; S- Session; NM- Null Model; P(M | data)- posterior model probability; BF_M - Bayes Factor comparing the best model to all others; R^2 - explained variance of the model. Results in bold reflect greater evidence with Session included.

For Maximum Power, Session was the main determinant ($BF_M = 5.525$), followed by a model including physical activity level ($BF_M = 3.477$), which provided weaker support. Post-hoc tests showed decisive differences between S1–S2 ($BF_{10,U} = 252.827$, $\epsilon < 0.001$) and S1–S3 ($BF_{10,U} = 373.998$, $\epsilon < 0.001$). A similar pattern was observed for Peak RPD, where the best model highlighted Session ($BF_M = 5.144$), with a secondary model including physical activity level receiving lower support ($BF_M = 3.077$). Post-hoc tests again showed strong session effects between S1–S2 ($BF_{10,U} = 37.625$, $\epsilon < 0.001$) and S1–S3 ($BF_{10,U} = 20.288$, $\epsilon < 0.001$).

In the remaining power- and velocity-related metrics results favored the null model.

Regarding the EMG-derived metrics, only EMG Rise Slope showed an effect of physical activity level ($BF_M = 4.876$), whereas the others were best explained by the null model.

5.2.1.1 Progression of Adaptation

The following results describe how the variables that demonstrated progressive increases across sessions evolved from Session 1 to Sessions 2 and 3, comparing their adaptation to the experimental stimuli.

For the bench press, paired-samples t-tests were applied to Maximum Power and Maximum Velocity. For Maximum Power under the ABF stimulus, the comparison across sessions yielded $BF_{-0} = 19.31$ ($\epsilon = 0.001$), providing very strong evidence for adaptation. In contrast, the GM stimulus produced only anecdotal evidence ($BF_{-0} = 1.706$, $\epsilon < 0.001$), suggesting that adaptation was minimal. For Maximum Velocity, results again favored ABF, with strong evidence of growth ($BF_{-0} = 9.198$, $\epsilon < 0.001$), whereas GM showed very weak support ($BF_{-0} = 1.287$, $\epsilon < 0.001$).

For the squat, paired-samples t-tests were performed on Maximum Power and Peak

RPD. For Maximum Power, both ABF ($BF_{-0} = 0.426$, $\epsilon < 0.001$) and GM ($BF_{-0} = 0.287$, $\epsilon < 0.001$) provided only anecdotal evidence, with GM showing even weaker support. Similarly, Peak RPD showed anecdotal evidence under both ABF ($BF_{-0} = 0.307$, $\epsilon = 0.007$) and GM ($BF_{-0} = 0.703$, $\epsilon < 0.001$), suggesting no substantial adaptation for this metric under either stimulus.

5.2.2 Female Participants Analysis

The results from the Bayesian two-way repeated-measures ANOVA for all metrics are presented in Table 5.5 in the bench press.

Table 5.5: Bayesian repeated-measures ANOVA results for all evaluated metrics in the bench press exercise among female participants.

Variables	Session						BestM	P(M data)	BF_M	R^2
	S1		S2		S3					
	ABF	GM	ABF	GM	ABF	GM				
Max Power (W)	69.6 ± 28.0	69.6 ± 28.2	70.6 ± 31.6	68.6 ± 28.9	68.7 ± 26.8	67.8 ± 28.8	PAL	0.648	16.534	0.705
Max Velocity (m/s^2)	0.7 ± 0.2	0.7 ± 0.2	0.7 ± 0.2	0.6 ± 0.2	0.7 ± 0.1	0.7 ± 0.2	PAL	0.471	8.021	0.682
Peak RPD (W/s)	129.1 ± 47.1	133.8 ± 63.1	134.0 ± 53.0	134.2 ± 50.5	129.2 ± 48.4	125.9 ± 48.0	PAL	0.465	7.810	0.742
PP Index (%)	45.5 ± 3.9	47.5 ± 6.1	46.0 ± 3.6	46.6 ± 4.5	46.0 ± 5.4	46.0 ± 5.9	NM	0.377	5.442	0.452
PV Index (%)	52.5 ± 3.9	54.9 ± 3.9	52.7 ± 4.3	53.0 ± 4.2	52.4 ± 4.8	52.1 ± 5.7	NM	0.328	4.401	0.514
Velocity Power Dif (ms)	33.0 ± 10.0	34.0 ± 13.0	30.0 ± 12.0	30.0 ± 10.0	29.0 ± 12.0	28.0 ± 12.0	PAL	0.292	3.710	0.441
TP Slope (W/s)	93.5 ± 35.1	96.4 ± 47.0	95.6 ± 38.9	96.1 ± 37.3	92.6 ± 36.1	90.4 ± 33.9	PAL	0.452	7.434	0.790
WP Slope (W/s)	103.6 ± 41.5	105.3 ± 49.5	105.6 ± 45.6	105.0 ± 43.2	102.5 ± 42.1	101.6 ± 40.9	PAL	0.501	9.037	0.796
Velocity Corr (-)	1.0 ± 0.1	1.0 ± 0.0	1.0 ± 0.1	1.0 ± 0.0	1.0 ± 0.0	1.0 ± 0.0	NM	0.311	4.064	0.785
ACC Corr (-)	1.0 ± 0.1	1.0 ± 0.0	0.9 ± 0.1	0.9 ± 0.1	1.0 ± 0.0	1.0 ± 0.1	NM	0.270	3.337	0.724
EMG Rise Time (s)	0.6 ± 0.2	0.6 ± 0.2	0.5 ± 0.2	0.6 ± 0.1	0.5 ± 0.2	0.5 ± 0.2	S	0.388	5.701	0.750
EMG Rise Slope (mV/s)	0.1 ± 0.1	0.1 ± 0.1	0.1 ± 0.1	0.1 ± 0.1	0.1 ± 0.1	0.1 ± 0.1	NM	0.346	4.769	0.879
EMG Onset to PP (s)	0.4 ± 0.1	0.4 ± 0.1	0.3 ± 0.0	0.4 ± 0.1	0.3 ± 0.0	0.3 ± 0.0	S	0.277	1.536	0.504
EMG Median Freq (Hz)	67.4 ± 10.6	66.2 ± 11.6	65.1 ± 11.2	65.6 ± 11.3	63.8 ± 11.5	66.2 ± 11.6	NM	0.562	5.124	0.800

Legend: Max- Maximum; RPD- Rate of Power Development; PP- Peak Power; PV- Peak Velocity; Dif- Difference; TP- Total Power; WP- Window Power; Corr- Correlation; ACC- Acceleration; Freq- Frequency; BestM- Best Model; S- Session; PAL- Physical Activity Level; NM- Null Model; P(M| data)- posterior model probability; BF_M - Bayes Factor comparing the best model to all others; R^2 - explained variance of the model. Results in bold reflect greater evidence with Session included.

For the bench press in women, the variability of Maximum Power, Maximum Velocity, Peak RPD, Velocity Power Difference, Total Power Slope, and Window Power Slope was explained by physical activity level ($BF_M \in [3.710-16.534]$), with moderate-to-strong evidence. In contrast, the remaining power- and velocity-related metrics were best explained by the null model, indicating the absence of systematic effects from the tested factors.

Among the EMG-derived metrics, Rise Time was most strongly explained by Session ($BF_M = 5.701$), with post-hoc tests revealing strong differences between S1–S3 ($BF_{10,U} = 20.137$, $\epsilon < 0.001$) and S2–S3 ($BF_{10,U} = 17.238$, $\epsilon < 0.001$). Figure 5.3 illustrates the decreasing trend of this metric across sessions.

EMG Onset to Peak Power was also best explained by Session ($BF_M = 1.536$), though the statistical evidence was insufficient to support a robust effect. Both EMG Rise Slope and EMG Median Frequency were favored by the null model.

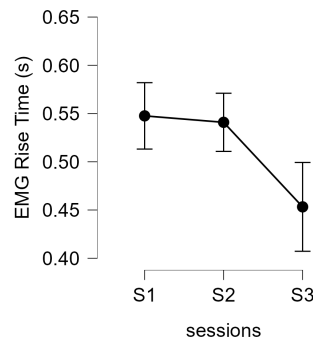


Figure 5.3: Evolution of EMG Rise Time across sessions in the bench press for women.

The results from the Bayesian two-way repeated-measures ANOVA for all metrics are presented in Table 5.6 in the squat.

Table 5.6: Bayesian repeated-measures ANOVA results for all evaluated metrics in the squat exercise among female participants.

Variables	Session						BestM	P(M data)	BF_M	R^2
	S1		S2		S3					
	ABF	GM	ABF	GM	ABF	GM				
Max Power (W)	218.4 ± 86.1	233.4 ± 91.6	228.7 ± 82.4	233.4 ± 83.4	225.8 ± 75.5	235.5 ± 93.8	NM	0.289	3.662	0.793
Max Velocity (m/s^2)	0.4 ± 0.1	0.5 ± 0.1	0.5 ± 0.1	0.5 ± 0.1	0.4 ± 0.1	0.5 ± 0.1	AS	0.295	3.771	0.559
Peak RPD (W/s)	329.1 ± 134.2	349.5 ± 152.0	337.8 ± 138.5	349.4 ± 148.1	323.9 ± 123.4	353.9 ± 152.0	NM	0.243	2.887	0.661
PP Index (%)	70.3 ± 6.7	70.3 ± 7.6	72.9 ± 7.6	74.8 ± 6.3	74.0 ± 6.3	72.0 ± 7.7	S+PAL	0.211	2.402	0.525
PV Index (%)	71.0 ± 6.1	71.2 ± 6.7	73.4 ± 7.0	75.2 ± 5.8	74.5 ± 5.9	72.5 ± 7.2	S+PAL	0.204	2.306	0.533
Velocity Power Dif (ms)	4.0 ± 3.0	6.0 ± 6.0	3.0 ± 5.0	2.0 ± 5.0	3.0 ± 4.0	3.0 ± 4.0	PAL	0.198	2.222	0.448
TP Slope (W/s)	162.8 ± 57.5	171.7 ± 63.5	145.8 ± 61.3	142.7 ± 69.0	139.9 ± 50.0	170.7 ± 114.8	NM	0.286	3.603	0.580
WP Slope (W/s)	169.7 ± 62.6	180.7 ± 70.2	152.0 ± 66.6	147.2 ± 72.4	144.9 ± 53.5	177.4 ± 122.3	NM	0.283	3.557	0.543
Velocity ACC (-)	0.9 ± 0.1	0.8 ± 0.2	0.8 ± 0.2	0.9 ± 0.1	0.8 ± 0.2	0.9 ± 0.2	NM	0.371	5.315	0.310
ACC Corr (-)	0.9 ± 0.1	0.9 ± 0.1	0.9 ± 0.1	1.0 ± 0.1	0.9 ± 0.1	1.0 ± 0.1	NM	0.270	3.336	0.260
EMG Rise Time (s)	0.4 ± 0.2	0.5 ± 0.3	0.5 ± 0.1	0.5 ± 0.1	0.4 ± 0.1	0.4 ± 0.2	NM	0.316	4.160	0.444
EMG Rise Slope (mV/s)	0.1 ± 0.1	0.1 ± 0.0	0.1 ± 0.1	0.1 ± 0.0	0.1 ± 0.0	0.1 ± 0.1	NM	0.335	4.533	0.576
EMG Onset to PP (s)	0.7 ± 0.1	0.7 ± 0.2	0.8 ± 0.2	0.8 ± 0.2	0.8 ± 0.3	0.8 ± 0.2	PAL	0.220	2.536	0.557
EMG Median Freq (Hz)	63.7 ± 7.6	68.2 ± 8.8	69.7 ± 10.5	69.2 ± 14.2	65.9 ± 9.5	66.9 ± 9.1	NM	0.204	2.303	0.365

Legend: Max- Maximum; RPD- Rate of Power Development; PP- Peak Power; PV- Peak Velocity; Dif- Difference; TP- Total Power; WP- Window Power; AS- Acoustic Stimulus; Corr- Correlation; ACC- Acceleration; Freq- Frequency; BestM- Best Model; S- Session; PAL- Physical Activity Level; NM- Null Model; P(M | data)- posterior model probability; BF_M - Bayes Factor comparing the best model to all others; R^2 - explained variance of the model; “+” indicates inclusion of main effects.

For Maximum Velocity, the best model ($BF_M = 3.771$) identified Acoustic Stimulus as the main factor, with the GM condition showing superior values compared to ABF. Peak Power Index and Peak Velocity Index were linked to Session and physical activity level but only with anecdotal evidence ($BF_M = 2.402$ and $BF_M = 2.306$). Similarly, Velocity Power Difference was best explained by physical activity level ($BF_M = 2.222$), though weakly supported. The remaining power- and velocity-related metrics favored the null model, indicating no substantial effects of the tested factors.

Regarding the EMG-derived metrics, all were best explained by the null model except for EMG Onset to Peak Power, where physical activity level emerged as the best predictor, though only with anecdotal evidence ($BF_M = 2.536$).

5.2.2.1 Progression of Adaptation

For women, only the variable EMG Rise Time during the bench press showed moderate evidence of differences across sessions, justifying an analysis of its adaptation to the auditory stimuli.

Results showed that, for ABF, the comparisons between Session 1–2 and Session 1–3 yielded $BF_{-0} = 0.130$ ($\epsilon < 0.001$), providing only anecdotal support. Under the GM stimulus, the same contrasts produced an even lower Bayes Factor ($BF_{-0} = 0.091$, $\epsilon < 0.001$), further reinforcing that the observed differences across sessions lacked sufficient statistical evidence.

5.3 Perceived Enjoyment with Auditory Stimuli

The Bayesian two-way repeated-measures ANOVA applied to PACES-8 scores across sessions and auditory stimuli, revealed moderate evidence for differences between stimuli ($BF_M = 6.184$). The best model consistently explained the variability of the outcome ($R^2 = 0.596$; $P(M|data) = 0.256$). Figure 5.4 shows the difference in perceived enjoyment between the two auditory stimuli across sexes.

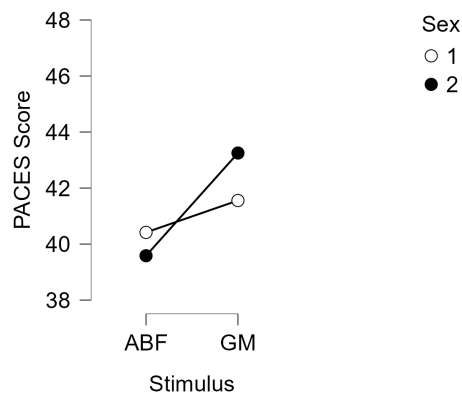


Figure 5.4: PACES-8 scores comparing perceived enjoyment between the ABF and GM auditory stimuli, stratified by sex. 1- Male; 2- Female.

DISCUSSION

This study aimed to evaluate the acute effects of EMG-based ABF on muscle power, intramuscular coordination, and subjective enjoyment in young adults. Participants performed the bench press and squat exercises at different loads (30–70% of 1RM for the bench press and 40–80% of 1RM for the squat) under two auditory conditions (ABF and GM) across three sessions.

The global analysis revealed distinct sex-related patterns. In the bench press, men showed progressive increases across sessions in power- and velocity-related metrics, while women's values remained more stable. Other indicators of intramuscular coordination and power also differed between sexes. In the squat, only limited progression in power metrics was observed, mostly in men, while some velocity and power-related measures showed disparities between sexes.

Beyond these overall results, the sex-stratified analysis made it possible to examine, within each sex, how the most relevant variables evolved through the quantification of their adaptation across sessions. Only men showed evident adaptations for power-related metrics in the bench-press, with greater improvements under ABF than GM.

Finally, participants reported that GM was perceived as more enjoyable than ABF, particularly among women.

In this discussion, only variables with a $P(M | \text{data})$ probability above 0.120 and an R^2 greater than 0.5 were considered, ensuring both statistical support and explanatory relevance.

6.1 Overall Analysis: Progression and Sex Differences

As previously noted, men showed a more pronounced progression than women in both the bench press and the squat, which may be explained by multiple factors.

Early gains in strength and power after only a few training sessions are largely attributable to neural adaptations [88], including improved motor unit recruitment, higher firing rates, and enhanced intramuscular coordination [89]. However, the greater improvements observed in men in this study may be linked to sex-related differences in motor

performance. Evidence suggests that pubertal changes in the central nervous system provide men an advantage in motor learning [90].

Biological differences further contribute to this divergence. Men generally exhibit a greater CSA and greater distribution of type II muscle fibers [91], which provides a structural advantage for generating high power outputs for short period [92]. This larger CSA represents a greater potential that can be exploited during the initial neural adaptations, possibly contributing to the more pronounced progression observed in men across the first testing sessions. In addition, higher testosterone levels in men can create a more favorable environment for high-intensity neural adaptation, promoting protein synthesis and neuromuscular explosiveness. Conversely, women's higher estrogen levels may support endurance and recovery adaptations, but are less directly aligned with rapid power development [93]. Moreover, fluctuations across the menstrual cycle can also influence neuromuscular function [94].

Experiential and behavioral aspects may also play a role. Men often have greater prior exposure to high-intensity and power-oriented training [95], which accelerates their learning curve in explosive tasks. In this study, most male participants were highly active, which may further explain their sharper progression. Finally, motivational factors are relevant: men are frequently driven by competition and strength outcomes, whereas women may emphasize consistency, supervision, and technical mastery [95]. Such tendencies could explain why women displayed more stable performance, while men prioritize immediate progression and maximal output, exhibiting faster improvements across sessions.

6.1.1 Bench Press: Sex-Based Performance Disparities

In addition to the observed progression in Maximum Power, Maximum Velocity and Peak RPD, men also achieved higher values in this metrics compared with women, in the bench press. This finding is consistent with previous research. In a recent cross-sectional study [96], a velocity-based training bench press test at different %1RM loads, normalized by body mass and fat-free mass, showed that men outperformed women in nearly all relative strength and power variables. These differences were attributed to a greater predominance of type II fibers, superior muscle quality, and higher glycolytic activity.

In this exercise, EMG Rise Time tended to decrease across sessions, with a more pronounced reduction in women. However, when relative differences were examined, this adaptation was not evident for either auditory condition, providing only anecdotal evidence of change. Also, the EMG Onset to Peak Power showed to varied with body mass.

Beyond this, the metrics Velocity Power Difference, Total Power Slope, and EMG Rise Slope also revealed marked sex-related disparities, a pattern consistent with previous work. Alonso-Aubin et al. [97] assessed male and female rugby players using force-velocity profiling in both the squat and bench press. They observed sex differences in the time to reach peak velocity and peak power (50–80% 1RM), supporting the view that temporal

dynamics differ between men and women.

Although Total Power Slope itself has not been previously studied, related insights can be drawn from research on the RFD. Men typically display higher absolute RFD values [98], but these differences diminish once normalized to maximal strength [99]. Unlike RFD, Total Power Slope reflects the combined progression of force and velocity, meaning that velocity dynamics are equally critical to the rate at which power rises. This may explain the sex-related disparities observed in this metric, beyond what is accounted for by RFD.

Regarding EMG Rise Slope, although the tasks differed, the cross-sectional study by Ives et al. [100] points in the same direction, reinforcing the presence of sex-related differences. The authors examined rapid elbow extension movements and found faster EMG rise in men, particularly in the triceps brachii, along with stronger reciprocal activation patterns, whereas women displayed more gradual activation strategies. The authors interpreted these findings as evidence that the higher EMG Rise Slope in men reflects a greater capacity for rapid neural modulation, particularly for abrupt and efficient antagonist activation during fast movements.

6.1.2 Squat: Sex-Based Performance Disparities

Beyond the progression observed in men for Maximum Power and Peak RPD, Maximum Velocity in the squat did not display a clear trend over time but did reveal sex-related differences. Previous research [97] reported sex differences in maximal squat velocity across all relative loads, with women achieving lower peak velocities and requiring more time to reach them. Sex-related disparities were also evident in the Total Power Slope and Window Power Slope metrics.

With respect to the observed values, the present findings are consistent with those reported in previous work [97] for Maximum Power and Maximum Velocity. In the present study, both Maximum Power and Peak RPD values were higher in men than in women and higher in the squat than in the bench press, reflecting the involvement of larger lower-limb muscle groups and their greater muscle mass, which provide enhanced capacity for force production. Prior research has shown that the VL, by virtue of being a larger muscle, contains a substantial number of fast-twitch fibers in absolute terms [101], and that leg muscles in general exhibit higher glycolytic potential compared with the triceps brachii [102]. By contrast, Maximum Velocity was lower in the squat than in the bench press. This is likely explained by the heavier loads and the greater technical and postural demands of the squat [103], [104], which constrain bar velocity and make it less responsive to short-term adaptations.

6.2 Adaptation Analyses

While the overall analysis showed no differences between stimuli, the sex-stratified results revealed that in men, and specifically in the bench press, adaptations appeared only in Maximum Power and Maximum Velocity, with greater improvements under the ABF condition.

Humans have a natural ability to follow auditory cues [105], and because in the ABF tool each contraction modifies the signal, participants can adjust their motor output in real time. Unlike GM, which provides only a general rhythm, ABF delivers task-specific information by mapping muscle activation to sound [7]. In the bench press, this performance-linked feedback likely contributed to the superior adaptations observed in men with ABF, whereas GM, although enjoyable, did not provide information that could directly guide execution.

By contrast, in the squat, no differences in adaptation between auditory conditions were observed for any metric. This may partly reflect men's stronger preference for upper-body over lower-body exercises [95], which could have increased engagement during the bench press. Another factor concerns the sonification design: as noted by Peres et al. [57], effectiveness depends on how well the auditory representation matches task demands. Since the sonification was originally developed from biceps brachii EMG, it was biomechanically more aligned with upper-limb actions such as the bench press than with lower-limb movements like the squat, favoring clearer effects in the former.

Physiological and biomechanical differences between the muscles further support this interpretation. In the bench press, the triceps brachii alternates between low activation in the eccentric phase and sharp peaks in the concentric phase, producing a highly discriminant EMG pattern and a clearer auditory signal [106], [107]. By contrast, during the squat, the quadriceps, particularly the VL, remain continuously active, generating a flatter EMG profile [106], [108] due to their pennate architecture and a greater relative proportion of slow-twitch fibers [109]. Conversely, the triceps, with a more fusiform structure and a higher relative proportion of fast-twitch fibers [109], supports sharper EMG peaks and faster contractions. These distinctions are consistent with participants' reports of perceiving ABF more clearly in the bench press than in the squat.

In women, bench press performance displayed relatively stable patterns across sessions. Discrepancies in Maximum Power, Maximum Velocity, Peak RPD, Total Power Slope, and Window Power Slope showed to stem from the heterogeneity in physical activity levels. Supporting this, Miller et al. [110] showed that trained women reached maximal power at lower relative loads and produced greater power at submaximal intensities than untrained women. Although no studies have directly examined RPD or power-curve slopes, it is reasonable to assume that similar neuromuscular adaptations underlie these variables, given their dependence on explosive force and velocity. In the squat, Maximum Velocity appeared to depend on the auditory condition, with higher values observed under GM compared to ABF. This effect can be explained by the fact that women benefit more from

melodic or emotionally arousing music while men respond more positively to rhythm-based auditory regulation of movement [111].

6.3 Limitations

In this study some limitations should be noted. First, physical activity levels were not controlled across participants. The male group was relatively homogeneous, with most reporting high activity levels, whereas the female group was more heterogeneous. This imbalance may have influenced responsiveness to the auditory stimulus. Moreover, the stable values observed in women may partly reflect that certain factors, such as menstrual cycle phases, were not considered, as hormonal fluctuations can affect neuromuscular function [94].

Second, selecting the VL as the target muscle may not have been optimal. Assessing the ABF stimulus in other muscles, such as the rectus femoris, and comparing meaningfulness across sites could have provided further insight. The sonification design itself could also have been more specifically tailored to each task.

Another limitation concerns the measurement tools. While squat angles were monitored in real time, no equivalent system was implemented for the bench press, which was guided only by verbal instruction. In addition, no device, such as a metronome, was used to control eccentric velocity. Although such measures could have increased methodological rigor, additional cues might also have interfered with the ABF, distracting participants from the main stimulus.

Finally, the acute design, with few sessions and short intervals between them, limited the potential to observe more pronounced effects, particularly in sEMG outcomes.

CONCLUSIONS AND FUTURE WORK

This study investigated the acute effects of EMG-based ABF on muscle power in young individuals, with the purpose of establishing a reference in a healthy population before extending applications to fragile groups such as the elderly.

The findings showed that, in men, ABF produced short-term adaptations in bench press performance, with improvements in Maximum Power and Maximum Velocity compared with GM. In women, no differences were observed between stimuli, as performance values remained stable across sessions and depended mainly on physical activity level.

Intramuscular coordination in upper and lower limbs did not display acute adaptations over the sessions nor between stimuli, likely due to the short duration of the intervention, but showed marked sex-related disparities.

Participants reported greater enjoyment with GM than with ABF in both sexes, suggesting that subjective perception is unrelated to performance across stimuli.

These results highlight the potential of EMG-based ABF as a valuable tool for enhancing power-oriented training. Its application may be further optimized by considering differences in sex and prior activity level, ensuring more effective and individualized strategies. To fully realize this potential, future studies should extend training duration to allow sufficient familiarization and adaptation to the ABF cues. In addition, refining the sonification system remains an important direction, as integrating alternative mechanical signals (e.g., velocity) could provide complementary cues that better capture movement dynamics and improve the meaningfulness and ecological validity of the feedback.

The observation of moderate-to-strong evidence after only three acute sessions suggests that longer interventions may further amplify ABF's benefits, reinforcing its potential as a power training aid. Observing positive outcomes in a healthy population indicates that ABF could benefit older adults, where age-related declines in muscle power impair physical function. Even when applied earlier, in adulthood, it may also help to delay or prevent such declines. Within the scope of the ASTROPOWER project, these findings point to ABF as a promising tool to combat powerpenia also seen in microgravity environments.

BIBLIOGRAPHY

- [1] J. M. Lourenço, *The NOVAthesis L^AT_EX Template User's Manual*, NOVA University Lisbon, 2021. [Online]. Available: <https://github.com/joaomlourenco/novathesis/raw/main/template.pdf> (cit. on p. i).
- [2] E. Wang, S. K. Nyberg, J. Hoff, *et al.*, "Impact of maximal strength training on work efficiency and muscle fiber type in the elderly: Implications for physical function and fall prevention," *Experimental gerontology*, vol. 91, pp. 64–71, 2017. DOI: <https://doi.org/10.1016/j.exger.2017.02.071> (cit. on pp. 1, 4).
- [3] A. T. Balachandran, J. Steele, D. Angielczyk, *et al.*, "Comparison of power training vs traditional strength training on physical function in older adults: A systematic review and meta-analysis," *JAMA network open*, vol. 5, no. 5, e2211623–e2211623, 2022. DOI: <https://doi.org/10.1001/jamanetworkopen.2022.11623> (cit. on pp. 1, 7).
- [4] S. R. Freitas, C. Cruz-Montecinos, S. Ratel, and R. S. Pinto, "Powerpenia should be considered a biomarker of healthy aging," *Sports Medicine-Open*, vol. 10, no. 1, p. 27, 2024. DOI: <https://doi.org/10.1186/s40798-024-00689-6> (cit. on pp. 1, 5).
- [5] R. Pellegrino, R. Paganelli, A. Di Iorio, *et al.*, "Role for neurological and immunological resilience in the pathway of the aging muscle powerpenia: Inchiante study longitudinal results," *GeroScience*, pp. 1–14, 2025. DOI: <https://doi.org/10.1007/s11357-025-01536-6> (cit. on pp. 1, 7).
- [6] G. V. Mendonca, P. Pezarat-Correia, J. R. Vaz, L. Silva, and K. S. Heffernan, "Impact of aging on endurance and neuromuscular physical performance: The role of vascular senescence," *Sports medicine*, vol. 47, pp. 583–598, 2017. DOI: <https://doi.org/10.1007/s40279-016-0596-8> (cit. on p. 1).
- [7] S. Pauletto and A. Hunt, "The sonification of emg data," *Proceedings of the 12th International Conference on Auditory Display*, pp. 152–157, 2006-01. [Online]. Available: https://www.researchgate.net/publication/303558586_The_sonification_of_EMG_data (cit. on pp. 1, 9, 38).

- [8] "Astro-power project." Accessed: 2025-08-27. (2025), [Online]. Available: <https://www.astro-power.eu> (cit. on p. 1).
- [9] P. Mil-Homens, P. P. Correia, and G. V. de Mendonça, Eds., *Treino da Força. Volume 1: Princípios Biológicos e Métodos de Treino*. Edições FMH, 2015 (cit. on pp. 3–5).
- [10] K. F. Reid and R. A. Fielding, "Skeletal muscle power: A critical determinant of physical functioning in older adult," *Exercise and sport sciences reviews*, vol. 40, no. 1, pp. 4–12, 2012. DOI: <https://doi.org/10.1097/JES.0b013e31823b5f13> (cit. on pp. 3, 5).
- [11] G. G. Haff and S. Nimphius, "Training principles for power," *Strength & Conditioning Journal*, vol. 34, no. 6, pp. 2–12, 2012. DOI: <https://doi.org/10.1519/SSC.0b013e31826db467> (cit. on p. 4).
- [12] C. Simpkins and F. Yang, "Muscle power is more important than strength in preventing falls in community-dwelling older adults," *Journal of biomechanics*, vol. 134, p. 111018, 2022. DOI: <https://doi.org/10.1016/j.jbiomech.2022.111018> (cit. on p. 4).
- [13] B. Simunic, H. Degens, J. Rittweger, M. Narici, I. Mekjavic, and R. Pisot, "Noninvasive estimation of myosin heavy chain composition in human skeletal muscle," *Medicine and science in sports and exercise*, vol. 43, no. 9, pp. 1619–1625, 2011. DOI: <https://doi.org/10.1249/MSS.0b013e31821522d0> (cit. on p. 4).
- [14] E. M. Castillo, D. Goodman-Gruen, D. Kritz-Silverstein, D. J. Morton, D. L. Wingard, and E. Barrett-Connor, "Sarcopenia in elderly men and women: The rancho bernardo study," *American journal of preventive medicine*, vol. 25, no. 3, pp. 226–231, 2003. DOI: [https://doi.org/10.1016/s0749-3797\(03\)00197-1](https://doi.org/10.1016/s0749-3797(03)00197-1) (cit. on p. 4).
- [15] V. Malafarina, F. Úriz-Otano, R. Iniesta, and L. Gil-Guerrero, "Sarcopenia in the elderly: Diagnosis, physiopathology and treatment," *Maturitas*, vol. 71, no. 2, pp. 109–114, 2012. DOI: <https://doi.org/10.1016/j.maturitas.2011.11.012> (cit. on p. 4).
- [16] J. Rice, J. Keogh, *et al.*, "Power training: Can it improve functional performance in older adults? a systematic review," *International Journal of Exercise Science*, vol. 2, no. 2, p. 6, 2009. DOI: <https://doi.org/10.70252/CULD5534> (cit. on pp. 4, 5).
- [17] B. C. Clark and T. M. Manini, "What is dynapenia?" *Nutrition*, vol. 28, no. 5, pp. 495–503, 2012. DOI: <https://doi.org/10.1016/j.nut.2011.12.002> (cit. on p. 4).
- [18] D. R. Claffin, L. M. Larkin, P. S. Cederna, *et al.*, "Effects of high-and low-velocity resistance training on the contractile properties of skeletal muscle fibers from young and older humans," *Journal of applied physiology*, vol. 111, no. 4, pp. 1021–1030, 2011. DOI: <https://doi.org/10.1152/jappphysiol.01119.2010> (cit. on p. 5).

- [19] S. P. Sayers, "High velocity power training in older adults," *Current Aging Science*, vol. 1, no. 1, pp. 62–67, 2008. DOI: <https://doi.org/10.1519/JSC.0b013e3182a361b8> (cit. on pp. 5, 6).
- [20] Y. Tsubouchi and K. Suzuki, "Biotones: A wearable device for emg auditory biofeedback," in *2010 Annual International Conference of the IEEE Engineering in Medicine and Biology*, IEEE, 2010, pp. 6543–6546. DOI: <https://doi.org/10.1109/IEMBS.2010.5627097> (cit. on pp. 5, 9).
- [21] J. Alcazar, P. Aagaard, B. Haddock, *et al.*, "Age-and sex-specific changes in lower-limb muscle power throughout the lifespan," *The Journals of Gerontology: Series A*, vol. 75, no. 7, pp. 1369–1378, 2020. DOI: <https://doi.org/10.1093/gerona/glaa013> (cit. on p. 6).
- [22] W. K. Mitchell, J. Williams, P. Atherton, M. Larvin, J. Lund, and M. Narici, "Sarcopenia, dynapenia, and the impact of advancing age on human skeletal muscle size and strength; a quantitative review," *Frontiers in physiology*, vol. 3, p. 260, 2012. DOI: <https://doi.org/10.3389/fphys.2012.00260> (cit. on p. 6).
- [23] J. Alcazar, C. Rodriguez-Lopez, C. Delecluse, M. Thomis, and E. Van Roie, "Ten-year longitudinal changes in muscle power, force, and velocity in young, middle-aged, and older adults," *Journal of cachexia, sarcopenia and muscle*, vol. 14, no. 2, pp. 1019–1032, 2023. DOI: <https://doi.org/10.1002/jcsm.13184> (cit. on p. 6).
- [24] C. G. S. Araújo, S. K. Kunutsor, T. M. Eijsvogels, *et al.*, "Muscle power versus strength as a predictor of mortality in middle-aged and older men and women," in *Mayo Clinic Proceedings*, Elsevier, 2025. DOI: <https://doi.org/10.1016/j.mayocp.2025.02.015> (cit. on p. 6).
- [25] E. J. Metter, R. Conwit, J. Tobin, and J. L. Fozard, "Age-associated loss of power and strength in the upper extremities in women and men," *The Journals of Gerontology Series A: Biological Sciences and Medical Sciences*, vol. 52, no. 5, B267–B276, 1997. DOI: <https://doi.org/10.1093/gerona/52a.5.b267> (cit. on p. 6).
- [26] C. Bosco and P. V. Komi, "Influence of aging on the mechanical behavior of leg extensor muscles," *European journal of applied physiology and occupational physiology*, vol. 45, no. 2, pp. 209–219, 1980. DOI: <https://doi.org/10.1007/BF00421329> (cit. on p. 6).
- [27] D. A. Skelton, C. A. Greig, J. M. Davies, and A. Young, "Strength, power and related functional ability of healthy people aged 65–89 years," *Age and ageing*, vol. 23, no. 5, pp. 371–377, 1994. DOI: <https://doi.org/10.1093/ageing/23.5.371> (cit. on p. 6).
- [28] S. Wiegmann, D. Felsenberg, G. Armbrecht, and R. Dietzel, "Longitudinal changes in muscle power compared to muscle strength and mass," *Journal of Musculoskeletal & Neuronal Interactions*, vol. 21, no. 1, p. 13, 2021. [Online]. Available: <https://pmc.ncbi.nlm.nih.gov/articles/PMC8020018/> (cit. on p. 6).

- [29] N. B. McKinnon, D. M. Connelly, C. L. Rice, S. W. Hunter, and T. J. Doherty, "Neuromuscular contributions to the age-related reduction in muscle power: Mechanisms and potential role of high velocity power training," *Ageing research reviews*, vol. 35, pp. 147–154, 2017. DOI: <https://doi.org/10.1016/j.arr.2016.09.003> (cit. on p. 7).
- [30] M. H. Rivner, T. R. Swift, and K. Malik, "Influence of age and height on nerve conduction," *Muscle & nerve*, vol. 24, no. 9, pp. 1134–1141, 2001. DOI: <https://doi.org/10.1002/mus.1124> (cit. on p. 7).
- [31] A. A. Vandervoort, "Aging of the human neuromuscular system," *Muscle & Nerve: Official Journal of the American Association of Electrodiagnostic Medicine*, vol. 25, no. 1, pp. 17–25, 2002. DOI: <https://doi.org/10.1002/mus.1215> (cit. on p. 7).
- [32] T. Hortobágyi, S. Solnik, A. Gruber, *et al.*, "Interaction between age and gait velocity in the amplitude and timing of antagonist muscle coactivation," *Gait & posture*, vol. 29, no. 4, pp. 558–564, 2009. DOI: <https://doi.org/10.1016/j.gaitpost.2008.12.007> (cit. on p. 7).
- [33] A. Schmitz, A. Silder, B. Heiderscheit, J. Mahoney, and D. G. Thelen, "Differences in lower-extremity muscular activation during walking between healthy older and young adults," *Journal of electromyography and kinesiology*, vol. 19, no. 6, pp. 1085–1091, 2009. DOI: <https://doi.org/10.1016/j.jelekin.2008.10.008> (cit. on p. 7).
- [34] V. Monaco and S. Micera, "Age-related neuromuscular adaptation does not affect the mechanical efficiency of lower limbs during walking," *Gait & posture*, vol. 36, no. 3, pp. 350–355, 2012. DOI: <https://doi.org/10.1016/j.gaitpost.2012.03.031> (cit. on p. 7).
- [35] S. Mosole, U. Carraro, H. Kern, *et al.*, "Long-term high-level exercise promotes muscle reinnervation with age," *Journal of Neuropathology & Experimental Neurology*, vol. 73, no. 4, pp. 284–294, 2014. DOI: <https://doi.org/10.1097/NEN.0000000000000032> (cit. on p. 7).
- [36] T. Suzuki, J. F. Bean, and R. A. Fielding, "Muscle power of the ankle flexors predicts functional performance in community-dwelling older women," *Journal of the American Geriatrics Society*, vol. 49, no. 9, pp. 1161–1167, 2001. DOI: <https://doi.org/10.1046/j.1532-5415.2001.49232.x> (cit. on p. 7).
- [37] A. Cuoco, D. M. Callahan, S. Sayers, W. R. Frontera, J. Bean, and R. A. Fielding, "Impact of muscle power and force on gait speed in disabled older men and women," *The Journals of Gerontology Series A: Biological Sciences and Medical Sciences*, vol. 59, no. 11, pp. 1200–1206, 2004. DOI: <https://doi.org/10.1093/gerona/59.11.1200> (cit. on p. 7).

- [38] M. Bottaro, S. N. Machado, W. Nogueira, R. Scales, and J. Veloso, "Effect of high versus low-velocity resistance training on muscular fitness and functional performance in older men," *European journal of applied physiology*, vol. 99, no. 3, pp. 257–264, 2007. DOI: <https://doi.org/10.1007/s00421-006-0343-1> (cit. on p. 8).
- [39] R. Orr, N. J. De Vos, N. A. Singh, D. A. Ross, T. M. Stavrinou, and M. A. Fiatarone-Singh, "Power training improves balance in healthy older adults," *The Journals of Gerontology Series A: Biological Sciences and Medical Sciences*, vol. 61, no. 1, pp. 78–85, 2006. DOI: <https://doi.org/10.1093/gerona/61.1.78> (cit. on p. 8).
- [40] T. A. Miszko, M. E. Cress, J. M. Slade, C. J. Covey, S. K. Agrawal, and C. E. Doerr, "Effect of strength and power training on physical function in community-dwelling older adults," *The Journals of Gerontology Series A: Biological Sciences and Medical Sciences*, vol. 58, no. 2, pp. M171–M175, 2003. DOI: <https://doi.org/10.1093/gerona/58.2.m171> (cit. on p. 8).
- [41] D. G. Behm, J. D. Young, J. H. Whitten, *et al.*, "Effectiveness of traditional strength vs. power training on muscle strength, power and speed with youth: A systematic review and meta-analysis," *Frontiers in physiology*, vol. 8, p. 423, 2017. DOI: <https://doi.org/10.3389/fphys.2017.00423> (cit. on p. 8).
- [42] H. F. Dorrell, M. F. Smith, and T. I. Gee, "Comparison of velocity-based and traditional percentage-based loading methods on maximal strength and power adaptations," *The Journal of Strength & Conditioning Research*, vol. 34, no. 1, pp. 46–53, 2020. DOI: <https://doi.org/10.1519/JSC.0000000000003089> (cit. on p. 8).
- [43] V. Sekulović, T. Jezdimirović-Stojanović, N. Andrić, *et al.*, "Effects of in-season velocity-based vs. traditional resistance training in elite youth male soccer players," *Applied Sciences*, vol. 14, no. 20, p. 9192, 2024. DOI: <https://doi.org/10.3390/app14209192> (cit. on p. 8).
- [44] M. Drey, A. Zech, E. Freiberger, *et al.*, "Effects of strength training versus power training on physical performance in prefrail community-dwelling older adults," *Gerontology*, vol. 58, no. 3, pp. 197–204, 2012. DOI: <https://doi.org/10.1159/000332207> (cit. on p. 8).
- [45] T. R. Henwood and D. R. Taaffe, "Improved physical performance in older adults undertaking a short-term programme of high-velocity resistance training," *Gerontology*, vol. 51, no. 2, pp. 108–115, 2005. DOI: <https://doi.org/10.1159/000082195> (cit. on p. 8).
- [46] M. Van Cutsem, J. Duchateau, and K. Hainaut, "Changes in single motor unit behaviour contribute to the increase in contraction speed after dynamic training in humans," *The Journal of physiology*, vol. 513, no. 1, pp. 295–305, 1998. DOI: <https://doi.org/10.1111/j.1469-7793.1998.295by.x> (cit. on p. 8).

- [47] Y. Liu, A. Schlumberger, K. Wirth, D. Schmidtbleicher, and J. M. Steinacker, "Different effects on human skeletal myosin heavy chain isoform expression: Strength vs. combination training," *Journal of Applied Physiology*, vol. 94, no. 6, pp. 2282–2288, 2003. DOI: <https://doi.org/10.1152/japplphysiol.00830.2002> (cit. on p. 8).
- [48] R. Radaelli, G. S. Trajano, S. R. Freitas, M. Izquierdo, E. L. Cadore, and R. S. Pinto, "Power training prescription in older individuals: Is it safe and effective to promote neuromuscular functional improvements?" *Sports Medicine*, vol. 53, no. 3, pp. 569–576, 2023. DOI: <https://doi.org/10.1007/s40279-022-01758-0> (cit. on p. 8).
- [49] P. Jaśkowski, K. Rybarczyk, F. Jaroszyk, and D. Lemański, "The effect of stimulus intensity on force output in simple reaction time task in humans," *Acta Neurobiologiae Experimentalis*, vol. 55, no. 1, pp. 57–64, 1995. DOI: <https://doi.org/10.55782/ane-1995-1061> (cit. on p. 8).
- [50] M. Murgia, F. Sors, R. Vono, *et al.*, "Using auditory stimulation to enhance athletes' strength: An experimental study in weightlifting," *Review of psychology*, vol. 19, no. 1, pp. 13–16, 2012. [Online]. Available: <https://hrcak.srce.hr/91392> (cit. on p. 9).
- [51] R. Ronsse, V. Puttemans, J. P. Coxon, *et al.*, "Motor learning with augmented feedback: Modality-dependent behavioral and neural consequences," *Cerebral cortex*, vol. 21, no. 6, pp. 1283–1294, 2011. DOI: <https://doi.org/10.1093/cercor/bhq209> (cit. on p. 9).
- [52] N. Hasegawa, K. Takeda, M. Mancini, L. A. King, F. B. Horak, and T. Asaka, "Differential effects of visual versus auditory biofeedback training for voluntary postural sway," *PloS one*, vol. 15, no. 12, e0244583, 2020. DOI: <https://doi.org/10.1371/journal.pone.0244583> (cit. on p. 9).
- [53] V. Lorenzoni, J. Staley, T. Marchant, K. E. Onderdijk, P.-J. Maes, and M. Leman, "The sonic instructor: A music-based biofeedback system for improving weightlifting technique," *Plos one*, vol. 14, no. 8, e0220915, 2019. DOI: <https://doi.org/10.1371/journal.pone.0220915> (cit. on p. 9).
- [54] L. Chiari, M. Dozza, A. Cappello, F. B. Horak, V. Macellari, and D. Giansanti, "Audio-biofeedback for balance improvement: An accelerometry-based system," *IEEE transactions on biomedical engineering*, vol. 52, no. 12, pp. 2108–2111, 2005. DOI: <https://doi.org/10.1109/TBME.2005.857673> (cit. on p. 9).
- [55] S. M. Lyons, T. M. Vickery, D. W. Powell, and M. R. Paquette, "Influence of auditory biofeedback of foot angular velocity on propulsive function and gait performance in old healthy adults," *Gait & Posture*, vol. 120, pp. 34–39, 2025. DOI: <https://doi.org/10.1016/j.gaitpost.2025.03.030> (cit. on p. 9).
- [56] Y. Nakayama, Y. Takano, M. Matsubara, K. Suzuki, and H. Terasawa, "The sound of smile: Auditory biofeedback of facial emg activity," *Displays*, vol. 47, pp. 32–39, 2017. DOI: <https://doi.org/10.1016/j.displa.2016.09.002> (cit. on p. 9).

- [57] S. C. Peres, D. Verona, T. Nisar, and P. Ritchey, "Towards a systematic approach to real-time sonification design for surface electromyography," *Displays*, vol. 47, pp. 25–31, 2017. DOI: <https://doi.org/10.1016/j.displa.2016.05.006> (cit. on pp. 9, 38).
- [58] J. Jonsdottir, D. Cattaneo, A. Regola, *et al.*, "Concepts of motor learning applied to a rehabilitation protocol using biofeedback to improve gait in a chronic stroke patient: An ab system study with multiple gait analyses," *Neurorehabilitation and neural repair*, vol. 21, no. 2, pp. 190–194, 2007. DOI: <https://doi.org/10.1177/1545968306290823> (cit. on p. 9).
- [59] E. Dursun, N. Dursun, and D. Alican, "Effects of biofeedback treatment on gait in children with cerebral palsy," *Disability and rehabilitation*, vol. 26, no. 2, pp. 116–120, 2004. DOI: <https://doi.org/10.1080/09638280310001629679> (cit. on p. 9).
- [60] Y.-J. Xie, S. Wang, Q.-J. Gong, *et al.*, "Effects of electromyography biofeedback for patients after knee surgery: A systematic review and meta-analysis," *Journal of Biomechanics*, vol. 120, p. 110386, 2021. DOI: <https://doi.org/10.1016/j.jbiomech.2021.110386> (cit. on p. 9).
- [61] J. Yang and A. Hunt, "Real-time auditory feedback of arm movement and emg in biceps curl training to enhance the quality," in *Proceedings of SoniHED—Conference on Sonification of Health and Environmental Data*, 2014. [Online]. Available: https://www.researchgate.net/publication/275824452_Real-time_Auditory_Feedback_of_Arm_Movement_and_EMG_in_Biceps_Curl_Training_to_Enhance_the_Quality (cit. on p. 9).
- [62] Heinrich Heine University Düsseldorf. "G*power: Statistical power analyses for windows and mac." Accessed: 2025-05-15. (2025), [Online]. Available: <https://www.psychologie.hhu.de/arbeitsgruppen/allgemeine-psychologie-und-arbeitspsychologie/gpower> (cit. on p. 10).
- [63] P. Teques, L. Calmeiro, C. Silva, and C. Borrego, "Validation and adaptation of the physical activity enjoyment scale (paces) in fitness group exercisers," *Journal of Sport and Health Science*, vol. 9, no. 4, pp. 352–357, 2020. DOI: <https://doi.org/10.1016/j.jshs.2017.09.010> (cit. on pp. 10, 12).
- [64] F. Rodrigues, P. Forte, D. S. Teixeira, L. Cid, and D. Monteiro, "The physical activity enjoyment scale (paces) as a two-dimensional scale: Exploratory and invariance analysis," *Montenegrin Journal of Sports Science and Medicine*, vol. 10, no. 1, pp. 61–66, 2021. DOI: <https://doi.org/10.26773/mjssm.210309> (cit. on p. 10).
- [65] H. M. P. G. Campaniço, "Validade simultânea do questionário internacional de actividade física através da medição objectiva da actividade física por actigrafia proporcional," M.S. thesis, Universidade de Lisboa (Portugal), 2016 (cit. on p. 11).

- [66] I. R. Committee, *Guidelines for the data processing and analysis of the international physical activity questionnaire (ipaq). short and long forms*, Accessed: 2025-08-16, 2005-11. [Online]. Available: <https://www.semanticscholar.org/paper/Guidelines-for-data-processing-analysis-of-the-and-Sjostrom-Ainsworth/efb9575f5c957b73c640f00950982e618e31a7be> (cit. on p. 11).
- [67] F. C. R. d. Santos *et al.*, "A relação da preferência e tolerância pela intensidade do exercício em praticantes recreacionais de crossfit," M.S. thesis, Universidade Lusófona, 2022. [Online]. Available: <https://research.ulusofona.pt/pt/studentTheses/a-rela%C3%A7%C3%A3o-da-prefer%C3%Aancia-e-toler%C3%Aancia-pela-intensidade-do-exerc%C3%ADc-5> (cit. on p. 11).
- [68] Tanita Europe, *Tanita bc-601 segmental body composition monitor*, Accessed: 2025-08-23, 2025. [Online]. Available: <https://tanita.eu/bc-601> (cit. on p. 11).
- [69] OSDUE, *Osdue electronic hand dynamometer*, Accessed: 2025-09-14, 2025. [Online]. Available: <https://www.amazon.co.uk/OSDUE-Electronic-Dynamometer-Measurement-Exerciser/dp/B0DHGVKGNX> (cit. on p. 11).
- [70] S. Europe, *Gym monster: All-in-one fitness studio, smart fitness trainer*. en, Accessed: 2025-01-30. [Online]. Available: https://eu.speediance.com/en/pages/gym-monster?gad_source=1&gclid=Cj0KCQiAhvK8BhDfARIsABsPy4gTDteql3bRR6oe1x09NrlZ4G_NlZyi6TxJelHeILZgVQZ3sDBs7BAaAsM8EALw_wcB (cit. on pp. 12, 64, 66, 67).
- [71] S. PLUX - Biosignals, en, Accessed: 2025-01-31. [Online]. Available: <https://www.pluxbiosignals.com/?srsltid=AfmBOopvdFG6JHEXHG8e1PVV1lkc844EpdUr0TSxhtmlJuzdcEa7Lh8-G> (cit. on p. 12).
- [72] C. Balsalobre, *My jump lab*, Accessed: 2025-09-28, 2025. [Online]. Available: <http://www.myjumplabpro.com/> (cit. on p. 12).
- [73] Seniam, *Surface electromyography for the non-invasive assessment of muscles (seniam)*, Accessed: 2025-09-17, 2025. [Online]. Available: <http://seniam.org/> (cit. on pp. 13, 60).
- [74] N. A. Ratamess, B. A. Alvar, T. K. Evetoch, *et al.*, "Progression models in resistance training for healthy adults," *Medicine & Science in Sports & Exercise: Official Journal of the American College of Sports Medicine*, vol. 41, no. 3, pp. 687–708, 2009. DOI: <https://doi.org/10.1249/MSS.0b013e3181915670> (cit. on pp. 14, 65).
- [75] PLUX Wireless Biosignals, *Electromyography (emg) sensor datasheet*, Accessed: 2025-07-16, 2021. [Online]. Available: <https://support.pluxbiosignals.com/wp-content/uploads/2021/10/biosignalsplux-Electromyography-EMG-Datasheet.pdf> (cit. on p. 15).

- [76] PLUX Wireless Biosignals, *Accelerometer (acc) sensor datasheet*, Accessed: 2025-07-16, 2021. [Online]. Available: https://support.pluxbiosignals.com/wp-content/uploads/2021/11/Accelerometer_ACC_Datasheet.pdf (cit. on p. 15).
- [77] B. Maczák, G. Vadai, A. Dér, I. Szendi, and Z. Gingl, "Detailed analysis and comparison of different activity metrics," *Plos one*, vol. 16, no. 12, e0261718, 2021. DOI: <https://doi.org/10.1371/journal.pone.0261718> (cit. on p. 15).
- [78] A. E. Hurtado-Perez, M. Toledano-Ayala, I. A. Cruz-Albarran, *et al.*, "Use of technologies for the acquisition and processing strategies for motion data analysis," *Biomimetics*, vol. 10, no. 5, p. 339, 2025. DOI: <https://doi.org/10.3390/biomimetics10050339> (cit. on p. 16).
- [79] SciPy Community, *Scipy documentation*, Accessed: 2025-08-23, 2025. [Online]. Available: <https://docs.scipy.org/doc/scipy/index.html> (cit. on p. 16).
- [80] M. M. Stadnyk, "Quantifying asymmetry and performance of lower limb mechanical muscle function in varsity athletes," 2019. DOI: <https://doi.org/10.7939/r3-gb9f-pw27> (cit. on p. 16).
- [81] S. Developers, *Stl decomposition — statsmodels documentation*, Accessed: 2025-08-23, 2025. [Online]. Available: https://www.statsmodels.org/dev/examples/notebooks/generated/stl_decomposition.html (cit. on p. 16).
- [82] L. R. Altimari, J. L. Dantas, M. Bigliassi, T. F. D. Kanthack, A. C. de Moraes, and T. Abrão, "Influence of different strategies of treatment muscle contraction and relaxation phases on emg signal processing and analysis during cyclic exercise," in *Computational Intelligence in Electromyography Analysis - A Perspective on Current Applications and Future Challenges*, G. R. Naik, Ed., London: IntechOpen, 2012, ch. 5. DOI: <https://doi.org/10.5772/50599> (cit. on p. 16).
- [83] G. Staude, C. Flachenecker, M. Daumer, and W. Wolf, "Onset detection in surface electromyographic signals: A systematic comparison of methods," *EURASIP Journal on Advances in Signal Processing*, vol. 2001, no. 2, p. 867853, 2001. DOI: <https://doi.org/10.1155/S1110865701000191> (cit. on p. 18).
- [84] JASP Team, *Jasp (version 0.95) [computer software]*, Accessed: 2025-09-5, 2020. [Online]. Available: <https://jasp-stats.org/> (cit. on p. 23).
- [85] D. McNeish, "On using bayesian methods to address small sample problems," *Structural Equation Modeling: A Multidisciplinary Journal*, vol. 23, no. 5, pp. 750–773, 2016. DOI: <https://doi.org/10.1080/10705511.2016.1186549> (cit. on p. 24).
- [86] R. E. Kass and A. E. Raftery, "Bayes factors," *Journal of the american statistical association*, vol. 90, no. 430, pp. 773–795, 1995. DOI: <https://doi.org/10.1080/01621459.1995.10476572> (cit. on p. 24).

- [87] PyMC Developers, *Bayes factor — pymc examples*, 2025-08-23, 2025. [Online]. Available: https://www.pymc.io/projects/examples/en/latest/diagnostics_and_criticism/Bayes_factor.html (cit. on p. 24).
- [88] A. Del Vecchio, A. Casolo, F. Negro, *et al.*, “The increase in muscle force after 4 weeks of strength training is mediated by adaptations in motor unit recruitment and rate coding,” *The Journal of physiology*, vol. 597, no. 7, pp. 1873–1887, 2019. DOI: <https://doi.org/10.1113/JP277250> (cit. on p. 35).
- [89] T. Moritani and H. A. DeVries, “Neural factors versus hypertrophy in the time course of muscle strength gain,” *American journal of physical medicine & rehabilitation*, vol. 58, no. 3, pp. 115–130, 1979. [Online]. Available: <https://pubmed.ncbi.nlm.nih.gov/453338/> (cit. on p. 35).
- [90] S. Dorfberger, E. Adi-Japha, and A. Karni, “Sex differences in motor performance and motor learning in children and adolescents: An increasing male advantage in motor learning and consolidation phase gains,” *Behavioural brain research*, vol. 198, no. 1, pp. 165–171, 2009. DOI: <https://doi.org/10.1016/j.bbr.2008.10.033> (cit. on p. 36).
- [91] J. L. Nuzzo, “Sex differences in skeletal muscle fiber types: A meta-analysis,” *Clinical anatomy*, vol. 37, no. 1, pp. 81–91, 2024. DOI: <https://doi.org/10.1002/ca.24091> (cit. on p. 36).
- [92] O. Vikmoen and B. R. Rønnestad, “A comparison of the effect of strength training on cycling performance between men and women,” *Journal of functional morphology and kinesiology*, vol. 6, no. 1, p. 29, 2021. DOI: <https://doi.org/10.3390/jfmk6010029> (cit. on p. 36).
- [93] K. Haizlip, B. Harrison, and L. Leinwand, “Sex-based differences in skeletal muscle kinetics and fiber-type composition,” *Physiology*, vol. 30, no. 1, pp. 30–39, 2015. DOI: <https://doi.org/10.1152/physiol.00024.2014> (cit. on p. 36).
- [94] P. Ansdell, C. G. Brownstein, J. Škarabot, *et al.*, “Menstrual cycle-associated modulations in neuromuscular function and fatigability of the knee extensors in eumenorrheic women,” *Journal of Applied Physiology*, vol. 126, no. 6, pp. 1701–1712, 2019. DOI: <https://doi.org/10.1152/jappphysiol.01041.2018> (cit. on pp. 36, 39).
- [95] J. L. Nuzzo, “Narrative review of sex differences in muscle strength, endurance, activation, size, fiber type, and strength training participation rates, preferences, motivations, injuries, and neuromuscular adaptations,” *The Journal of Strength & Conditioning Research*, vol. 37, no. 2, pp. 494–536, 2023. DOI: <https://doi.org/10.1519/JSC.0000000000004329> (cit. on pp. 36, 38).
- [96] O. López-Torres, R. Nieto-Acevedo, A. Guadalupe-Grau, and V. E. F. Elías, “Sex differences in bench press strength and power: A velocity-based analysis adjusted for body composition,” *Journal of Functional Morphology and Kinesiology*, vol. 10, no. 3, p. 284, 2025. DOI: <https://doi.org/10.3390/jfmk10030284> (cit. on p. 36).

- [97] D. A. Alonso-Aubin, I. Chulvi-Medrano, J. M. Cortell-Tormo, M. Picón-Martínez, T. R. Rebullido, and A. D. Faigenbaum, "Squat and bench press force-velocity profiling in male and female adolescent rugby players," *The Journal of Strength & Conditioning Research*, vol. 35, S44–S50, 2021. DOI: <https://doi.org/10.1519/JSC.0000000000003336> (cit. on pp. 36, 37).
- [98] D. G. Bell and I. Jacobs, "Electro-mechanical response times and rate of force development in males and females," *Medicine and science in sports and exercise*, vol. 18, no. 1, pp. 31–36, 1986. [Online]. Available: <http://europepmc.org/abstract/MED/3959861> (cit. on p. 37).
- [99] R. Hannah, C. Minshull, M. W. Buckthorpe, and J. P. Folland, "Explosive neuromuscular performance of males versus females," *Experimental physiology*, vol. 97, no. 5, pp. 618–629, 2012. DOI: <https://doi.org/10.1113/expphysiol.2011.063420> (cit. on p. 37).
- [100] J. C. Ives, W. P. Kroll, and L. L. Bultman, "Rapid movement kinematic and electromyographic control characteristics in males and females," *Research Quarterly for Exercise and Sport*, vol. 64, no. 3, pp. 274–283, 1993. DOI: <https://doi.org/10.1080/02701367.1993.10608811> (cit. on p. 37).
- [101] V. R. Edgerton, J. Smith, and D. Simpson, "Muscle fibre type populations of human leg muscles," *The Histochemical Journal*, vol. 7, no. 3, pp. 259–266, 1975. DOI: <https://doi.org/10.1007/BF01003594> (cit. on p. 37).
- [102] N. Ørtenblad, J. Nielsen, R. Boushel, K. Söderlund, B. Saltin, and H.-C. Holmberg, "The muscle fiber profiles, mitochondrial content, and enzyme activities of the exceptionally well-trained arm and leg muscles of elite cross-country skiers," *Frontiers in physiology*, vol. 9, p. 1031, 2018. DOI: <https://doi.org/10.3389/fphys.2018.01031> (cit. on p. 37).
- [103] G. D. Myer, A. M. Kushner, J. L. Brent, *et al.*, "The back squat: A proposed assessment of functional deficits and technical factors that limit performance," *Strength & Conditioning Journal*, vol. 36, no. 6, pp. 4–27, 2014. DOI: <https://doi.org/10.1519/SSC.000000000000103> (cit. on p. 37).
- [104] B. J. Schoenfeld, "Squatting kinematics and kinetics and their application to exercise performance," *The Journal of Strength & Conditioning Research*, vol. 24, no. 12, pp. 3497–3506, 2010. DOI: <https://doi.org/10.1519/JSC.0b013e3181bac2d7> (cit. on p. 37).
- [105] B. H. Repp and Y.-H. Su, "Sensorimotor synchronization: A review of recent research (2006–2012)," *Psychonomic bulletin & review*, vol. 20, no. 3, pp. 403–452, 2013. DOI: <https://doi.org/10.3758/s13423-012-0371-2> (cit. on p. 38).

- [106] PT Direct, *Skeletal muscle roles and contraction types*, Accessed: 2025-09-15, 2025. [Online]. Available: <https://www.ptdirect.com/training-design/anatomy-and-physiology/skeletal-muscle-roles-and-contraction-types> (cit. on p. 38).
- [107] D. D. Dunnick, L. E. Brown, J. W. Coburn, S. K. Lynn, and S. R. Barillas, "Bench press upper-body muscle activation between stable and unstable loads," *The Journal of Strength & Conditioning Research*, vol. 29, no. 12, pp. 3279–3283, 2015. DOI: <https://doi.org/10.1519/JSC.0000000000001198> (cit. on p. 38).
- [108] M. Murawa, A. Fryzowicz, J. Kabacinski, *et al.*, "Muscle activation varies between high-bar and low-bar back squat," *PeerJ*, vol. 8, e9256, 2020. DOI: <https://doi.org/10.7717/peerj.9256> (cit. on p. 38).
- [109] G. Sjøgaard, "Capillary supply and cross-sectional area of slow and fast twitch muscle fibres in man," *Histochemistry*, vol. 76, no. 4, pp. 547–555, 1982. DOI: <https://doi.org/10.1007/BF00489909> (cit. on p. 38).
- [110] R. M. Miller, E. D. Freitas, A. D. Heishman, *et al.*, "Maximal power production as a function of sex and training status," *Biology of sport*, vol. 36, no. 1, pp. 31–37, 2019. DOI: <https://doi.org/10.5114/biolsport.2018.78904> (cit. on p. 38).
- [111] C. I. Karageorghis, D. Priest, L. Williams, R. Hirani, K. Lannon, and B. Bates, "Ergogenic and psychological effects of synchronous music during circuit-type exercise," *Psychology of Sport and Exercise*, vol. 11, no. 6, pp. 551–559, 2010. DOI: <https://doi.org/10.1016/j.psychsport.2010.06.004> (cit. on p. 39).
- [112] P. Mil-Homens, P. P. Correia, and G. Mendonça, *Treino de Força, Volume 2: Avaliação, Planeamento e Aplicações*. FMH Edições, 2017 (cit. on p. 57).

| A

INFORMED CONSENT



Informação ao Participante e Consentimento informado, esclarecido e livre para participação em estudos de investigação

Por favor, leia com atenção a seguinte informação. Se achar que algo está incorreto ou que não está claro, não hesite em solicitar mais informações.

Título do estudo: “Estudo do efeito agudo de estímulos auditivos para otimizar a produção de potência muscular durante o exercício físico.”

Enquadramento: No âmbito do projeto ASTROPOWER (<https://astro-power.eu/>), levado a cabo pelo laboratório de bio-sinais do LIBPhys-UNL.

O investigador responsável Hugo Gamboa atuará como responsável pelo tratamento dos dados pessoais, no sentido em que tais expressões são mencionadas no Regulamento Geral sobre a Proteção de Dados.

Explicação do estudo: Este estudo envolve a recolha de dados fisiológicos dos músculos através de sensores de EMG, da atividade do coração através de um sensor ECG e de movimento através de um sensor de acelerometria e de força. A aquisição será nas instalações da Faculdade de Ciências e Tecnologias da Universidade NOVA de Lisboa. As aquisições serão feitas 3 vezes, durante aproximadamente uma hora e quinze minutos.

Será realizada uma sessão prévia (baseline) destinada à recolha de métricas fisiológicas e de desempenho físico, onde também será efetuada uma breve apresentação do projeto com os investigadores e esclarecimento de eventuais dúvidas. Antes desta sessão, os participantes devem preencher um questionário de caracterização da população, relativo à realização de atividade física. No final do estudo cada participante receberá um relatório que se baseia nos dados recolhidos dos sensores e nas medidas de composição corporal. É importante mencionar que neste relatório integrará os seus dados pessoais, dos quais é o único proprietário, pelo que não deve ser partilhado com ninguém. Condições: É importante referir que terá toda a liberdade para recusar a participação no estudo ou retirar o seu consentimento, suspendendo a participação em qualquer momento. Ao longo de todo o processo não terá qualquer custo por participar neste estudo. Os participantes neste estudo comprometem-se a cumprir os requisitos abaixo:

- Adultos com idade entre os 18 e os 29 anos.
- Indivíduos sem patologia neurológica, reumática, oncológica ou cardiorrespiratória.
- Audição funcional preservada, adequada à receção de estímulos sonoros.
- Indivíduos que não estejam a tomar medicamentos psicotrópicos.
- Indivíduos com capacidades motoras e cognitivas capazes de utilizar o equipamento necessário.
- Voluntários que não estejam de férias ou ausentes durante o período de recolha.



Confidencialidade e anonimato: Os dados pessoais recolhidos serão utilizados apenas no contexto desta investigação, não sendo divulgados em nenhum outro contexto. Dados anonimizados (i.e., biossinais e dados demográficos) poderão ser tornados públicos (publicações científicas e conferências).

Para assegurar que os seus dados pessoais são armazenados apenas durante o período necessário, e considerando o objetivo da investigação; os seus dados pessoais (como é o caso do nome e e-mail), serão armazenados em segurança durante um período de 1 ano após o fim do estudo, por motivos de possibilidade de contactar algum participante, caso necessário.

A qualquer momento, poderá exercer os seus direitos, nomeadamente o direito de solicitar mais informações sobre o tratamento dos seus dados pessoais, o direito de retificação e de apagamento de dados, de remoção do seu consentimento ou de oposição às atividades de tratamento, entre outros, de acordo com o disposto no Regulamento Geral sobre a Proteção de Dados.

Pode exercer os seus direitos contactando Hugo Filipe Silveira Gamboa, hgamboa@fct.unl.pt. Caso entenda que o tratamento dos seus dados pessoais não cumpre com a legislação aplicável têm, ainda, o direito de apresentar uma reclamação junto da autoridade supervisora competente. Em Portugal, pode contactar a Comissão Nacional de Proteção de Dados (CNPd) em <https://www.cnpd.pt/>.

Identificação do Investigador que irá recolher os dados:

Nome: Hugo Gamboa

Profissão: Professor e investigador principal do projeto

Contacto telefónico: 962 611 197

Endereço eletrónico: hgamboa@fct.unl.pt

Investigador

Confirmando que expliquei à pessoa abaixo indicada, de forma adequada e inteligível, os procedimentos necessários ao estudo referido neste documento. Respondi a todas as questões que me foram colocadas e assegurei-me de que houve um período de reflexão suficiente para a tomada da decisão.

(Assinatura Legível) _____

(Hugo Filipe Silveira Gamboa)

Data: ____ / ____ / ____



Participante

Por favor, leia com atenção todo o conteúdo deste documento. Não hesite em solicitar mais informações se não estiver completamente esclarecido(a). Verifique se todas as informações estão corretas. Se concordar com o procedimento descrito e com todas as informações fornecidas acerca do estudo e pretender continuar, por favor, assine em baixo.

Eu, abaixo-assinado (nome completo do voluntário)

declaro não estar a participar em nenhum outro projeto de investigação neste momento. Recebi o texto de *Informação ao Participante* referente ao procedimento que concordei em efetuar. Compreendi a explicação que me foi fornecida pelo investigador que assina este documento. Foi-me ainda dada oportunidade de fazer as perguntas que julguei necessárias, e de todas obtive resposta satisfatória.

Tomei conhecimento de que, de acordo com as recomendações da Declaração de Helsínquia, a informação ou explicação que me foi prestada versou os objetivos, os métodos, os benefícios previstos, os riscos potenciais e o eventual desconforto. Adicionalmente, foi-me afirmado que tenho o direito de cessar a minha participação no estudo, a qualquer momento, bem como pedir a imediata eliminação de todos os meus dados recolhidos no âmbito do estudo, sem que isso possa ter como efeito qualquer prejuízo na assistência que me é prestada.

Por isso, consinto de forma livre e esclarecida que me seja aplicado o método, o tratamento ou o inquérito proposto pelo investigador.

Assinatura do voluntário:

Data: / /

Nome e assinatura do Investigador responsável:

Data: / /

Anulação do Consentimento informado

Declaro que recebi a Informação ao participante referente ao estudo/projeto de investigação em questão, que me foi proposto pelo investigador que assina este documento e pretendo anular o consentimento dado na data / / .

Assinatura do voluntário:

Data: / /

Assinatura do Investigador responsável:

Data: / /

SUBMAXIMAL TEST FOR 1RM ESTIMATION

This chapter presents the submaximal protocol used to estimate the 1RM for the bench press and squat exercises.

B.1 Maximal Strength Assessment

Maximal strength for both the bench press and squat was assessed using a submaximal 1RM prediction test. This protocol estimates the 1RM indirectly, based on the number of repetitions performed with a predetermined submaximal load [112].

1. The warm-up should consist of 10 repetitions performed without any external load. After the warm-up, the exercise should begin with a load equivalent to 65% of body mass for female participants and 80% of body mass for male participants, for both exercises. These values may be adjusted based on the participant's physical condition and capacity.
2. Allow a 1-minute rest interval after the warm-up set.
3. Progressively increase the load by approximately 5 to 10% of the estimated maximum.
4. Instruct the participant to perform as many repetitions as possible with proper form, until volitional fatigue or technical failure.
5. Ensure the chosen load allows for no more than 10 repetitions.
6. If the participant completes more than 10 repetitions, the load should be increased and the attempt repeated after a 1-minute rest period.
7. Once the participant completes a valid set with 1 to 10 repetitions, use the corresponding prediction coefficient (table B.1), based on the number of repetitions performed to estimate the 1-RM:

$$\text{Predicted 1RM} = \text{Load lifted} \times \text{Coefficient}$$

APPENDIX B. SUBMAXIMAL TEST FOR 1RM ESTIMATION

Table B.1: Coefficients of prediction of 1RM based on the number of repetitions. Adapted from Baechle & Groves (1992).

Number of Repetitions (REP)	Coefficients
1	1.00
2	1.07
3	1.10
4	1.13
5	1.16
6	1.20
7	1.23
8	1.27
9	1.32
10	1.36

8. The test is concluded once a reliable value is obtained within the 1–10 repetition range, using correct technique and full range of motion.

EXPERIMENTAL PROTOCOL

This chapter outlines the experimental protocol applied in the study, describing the procedures for participant preparation, instrumentation, and training plan to ensure consistency and replicability.

C.1 Preparation (2 min)

Before starting any procedure, it is essential to ensure that the participant is properly prepared and equipped both for the physical activity and for the correct placement of the sensors. To guarantee safety, comfort, and the accuracy of the data collected, the following guidelines must be strictly observed:

- Clothing should be comfortable, preferably a t-shirt and shorts, to facilitate the placement of the sensors on the skin.
- Proper footwear is essential to provide stability and safety during exercise performance, reducing the risk of injury and optimizing performance.
- Watches, bracelets, or other accessories that may interfere with the sensors should be avoided.

C.2 Placement of Instruments (10 min)

C.2.1 Required Materials and Connection to BioPlux

The following sensors were used:

- 2 EMG sensors.
- 1 ACC sensor.
- 1 ECG sensor.
- 1 load cell.

All sensors were connected to a single *BioSignals by Plux* device with 8 channels, following the configuration shown in Figure C.1:

- Each sensor was connected to its corresponding port, considering the requirements of each type of device (e.g., accelerometers require three ports, whereas EMG sensors use only one).
- Cable organization was arranged to minimize interference and avoid restricting the participant's movements.

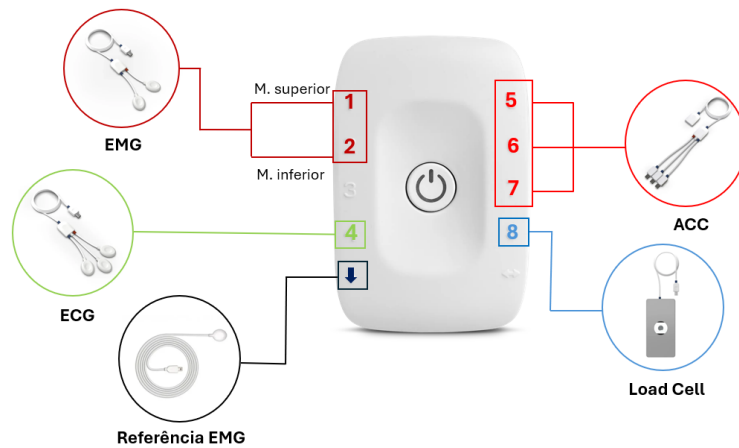


Figure C.1: Sensor arrangement in the BioPlux device.

C.2.2 Skin Preparation

For surface sensors, it is essential to properly prepare the skin to ensure clear signal acquisition free from interference. Hair in the region should be removed with a razor, followed by cleaning with a disinfectant solution. The skin should become slightly reddened, indicating effective preparation. Finally, the area must be clean and dry to guarantee proper electrode adhesion and to avoid failures in the acquisition of physiological signals.

C.2.3 Sensor Placement

At this stage, it is essential to ensure the correct application of the electrodes to guarantee accurate and reliable data collection, minimizing interference and optimizing the quality of the obtained signals.

C.2.3.1 EMG

If this is the first time performing the procedure or if there are doubts regarding sensor placement, it is recommended to consult the *Seniam* website [73], which provides detailed reference points for electrode positioning in each muscle.

It is important to consider individual variations in the muscular anatomy of each participant.

- For each muscle, two measurement electrodes should be used, positioned parallel to the orientation of the muscle fibers and placed over the muscle belly to ensure effective signal acquisition.
- To facilitate placement, it is advisable to ask the participant to contract the muscle in order to better visualize its anatomy. If necessary, perform flexion or extension against resistance.
- Although the order of the electrodes is not relevant, the distance between them should not exceed 20 mm, and they should be positioned as close as possible within this limit.
- Electrodes should only be placed on the right-side limbs.

EMG – Triceps Brachii: For the correct placement of the EMG sensors on the triceps brachii, the electrodes should be positioned at 50% of the line between the posterior crest of the acromion and the olecranon, at a distance of two finger-widths medially from this line.

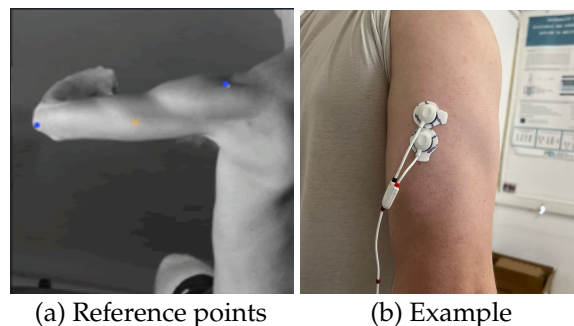


Figure C.2: EMG – Triceps Brachii.

EMG – Vastus Lateralis: For the correct placement of EMG sensors on the vastus lateralis, the electrodes should be positioned at two-thirds of the line between the anterior superior iliac spine and the lateral border of the patella.

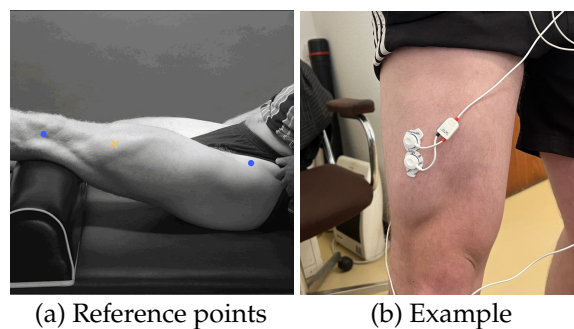


Figure C.3: EMG – Vastus Lateralis.

C.2.3.2 ECG

The ECG sensor used allows the acquisition of a single-lead electrocardiogram. Before starting the signal acquisition, it is crucial to ensure the correct placement of the electrodes, as illustrated in Figure C.4. The reference points for electrode placement are the following:

- **ST (Sternum):** Positioned below the sternum, close to the midline of the body.
- **LC (Left Chest):** Positioned below the left chest, near the nipple.
- **M (Manubrium):** Positioned on the manubrium, the prominent upper portion of the sternum.

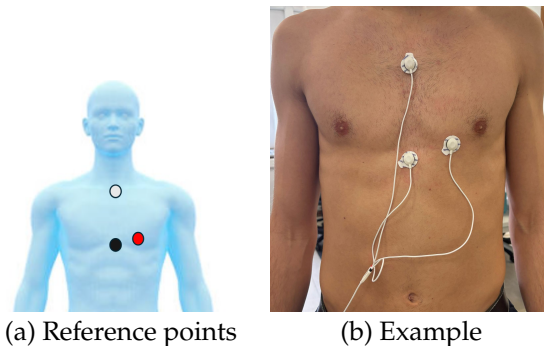


Figure C.4: Recommended ECG electrode positions.

Table C.1: ECG lead configuration.

	POSITIVE (+)	NEGATIVE (-)	REFERENCE
LEAD	ST	LC	M

C.2.4 ACC and Load Cell

The triaxial accelerometer and load cell sensors were previously attached to the bar of the training machine. The accelerometer was placed under the load cell, aligning its z-axis with the direction of movement. The sensors were positioned to minimize mechanical noise resulting from the bar's movement during exercises.

C.2.5 Connection to the BioPlux

After the correct placement of the sensors, they must be connected to the *BioPlux* device and to the custom *Pyhton* program to ensure the acquisition of physiological signals.

- Before starting data collection, it is essential to check all connections to ensure that signals are being captured correctly and that no noise or transmission failures are present.

- Pay attention to the chosen sampling rates and confirm that the signal type selected on the computer has been properly predefined.

C.3 Resting Measurements (2 min)

At this stage, baseline data collection is performed before the beginning of the training session, while the participant is at rest. The data and parameters to be collected are:

- Baseline heart rate (ECG).
- Resting muscle activity (EMG).
- Baseline ACC.

C.4 Start of Training

Before beginning the training session, a detailed explanation should be provided regarding the purpose of the session, the exercises to be performed with a description of their correct execution, the main muscle groups involved, and the precautions to be taken to prevent injuries. Practical demonstrations should be provided whenever necessary, and participants' questions should be clarified to ensure proper understanding and execution of the movements.

C.4.1 Required Training Materials

The following materials were used:

- Barbell.
- Bench.
- Earphones.

C.4.2 Activation (10 min)

C.4.2.1 Joint Warm-Up

Joint activation is a fundamental component of the warm-up, designed to mobilize and prepare the joints for the movements required during training. This stage lasts approximately 10 minutes and consists of the following six exercises:

- **Neck rotation:** Standing position, perform neck rotations — 10 repetitions to each side.
- **Wrist rotation:** Standing position, perform external and internal wrist rotations — 10 repetitions to each side.

- **Ankle rotation:** Standing position, place the tip of one foot on the floor and perform external and internal ankle rotations — 10 repetitions to each side; then repeat with the other foot.
- **Shoulder rotation:** Standing position, rotate both arms forward — 10 repetitions to each side. Rest for 10 seconds and repeat the movement backward.
- **Hip rotation:** Standing position, perform hip rotations — 10 repetitions to each side. Rest for 10 seconds between directions.
- **Knee rotation:** Standing position, feet together and knees slightly flexed, perform circular movements with the knees — 10 repetitions to each side.



Figure C.5: Shoulder rotation. Adapted from [70].

C.4.2.2 Exercise-Specific Warm-Up

As part of the warm-up, since the power test exercises were performed in the order of bench press followed by squat, participants completed 10 repetitions with a moderate load before each exercise. The load was defined according to each subject’s previous experience and individual capacity. This warm-up also served to refine the exercise technique, which had already been introduced during the maximal strength test in the baseline session.

C.4.3 Training Plan (50 min)

The training protocol consisted of two main exercises: the bench press and the squat. After the warm-up, participants performed a power test at multiple relative loads based on the 1RM values estimated during the baseline session. All repetitions were executed with maximal intended velocity during the concentric phase.

C.4.3.1 Bench Press Protocol

Participants performed five sets of three repetitions at the following relative loads:

Table C.2: Bench press protocol based on estimated 1RM values.

Exercise	Sets	Repetitions	Load (%1RM)
Bench Press	5	3	30, 40, 50, 60, 70

C.4.3.2 Squat Protocol

For the squat, participants also performed five sets of three repetitions, at slightly higher relative loads:

Table C.3: Squat protocol based on estimated 1RM values.

Exercise	Sets	Repetitions	Load (%1RM)
Squat	5	3	40, 50, 60, 70, 80

C.4.3.3 Auditory Conditions and Randomization

Each exercise was performed under two auditory conditions, presented in a randomized order:

- **ABF:** Acoustic biofeedback condition.
- **GM:** Predefined rhythmic music.

Randomization was applied independently for each exercise. For the bench press, participants first completed all five sets under one auditory condition (ABF or GM), and then repeated the sets under the other condition. For the squat, the order of auditory conditions was randomized again and could differ from the bench press sequence. The sequence of load intensities was also randomized within each exercise to minimize order and learning effects.

C.4.3.4 Rest Intervals

Each set consisted of three consecutive repetitions. A rest interval of 2 minutes was allowed between sets, and 3 minutes between exercises, in accordance with the recommendations of the ACSM [74], in order to minimize the accumulated fatigue.

C.5 Correct Execution of the Exercises

C.5.1 Squat

The squat is one of the fundamental exercises for developing lower-limb strength, primarily recruiting the quadriceps, hamstrings, and gluteal muscles.

- The bar should be positioned evenly across the trapezius.
- During execution, the participant should maintain the feet shoulder-width apart with a slight external rotation.
- The spine should remain neutral, and the eccentric phase should be controlled until the thighs are parallel to the ground.

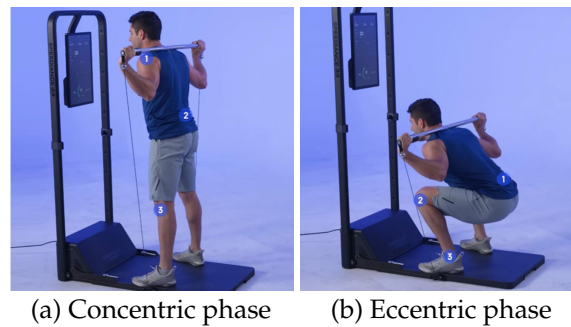


Figure C.6: Squat – *Speediance*. Adapted from [70].

C.5.2 Bench Press

The bench press is an essential exercise for developing the strength of the pectoralis major, anterior deltoids, and triceps brachii.

- The participant should lie on the bench with the feet firmly on the floor, holding the bar with a grip slightly narrower than shoulder-width to increase triceps involvement.
- The bar should be lowered in a controlled manner until it lightly touches the chest, followed by full elbow extension.
- A slight lumbar arch is allowed, provided the glutes remain in contact with the bench, and the scapulae should be retracted to avoid unnecessary shoulder overload.

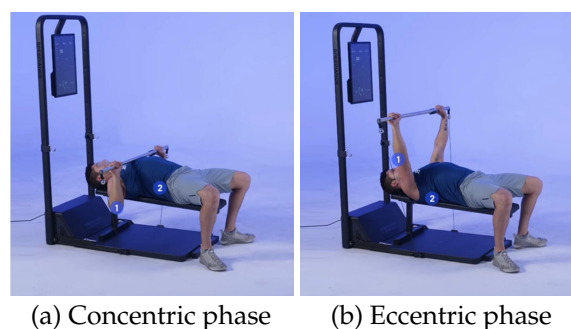


Figure C.7: Bench Press – *Speediance*. Adapted from [70].

C.6 Stretching

Simple stretching exercises were performed for 30 seconds per arm and 30 seconds per leg (approximately 3 minutes in total), focusing on the main muscle groups involved in the training session. During execution, participants were instructed to maintain controlled breathing and avoid sudden movements, ensuring a gradual and effective stretch.



(a) Arms



(b) Legs

Figure C.8: Stretching. Adapted from [70].

C.7 Cool-Down (4 min)

After completing the training session, participants engaged in a cool-down phase. This stage aimed to allow the body to gradually recover from physical exertion by normalizing cardiovascular, respiratory, and muscular functions. During the cool-down, it was essential to progressively reduce activity intensity, helping to avoid sudden cardiovascular stress and to promote the clearance of accumulated metabolic by-products such as lactic acid.

C.7.1 Walking

Participants walked for approximately 2 minutes at a comfortable pace.

C.7.2 Rest

The participant remained at rest for approximately 2 minutes to allow for physiological stabilization, during which signal acquisition was continued.

C.8 Equipment Removal (10 min)

- Save the acquired signal files.
- Carefully remove the sensors to avoid discomfort.
- Dispose of the used electrodes.
- Sanitize the earphones.
- Sanitize the bench.
- Store the instruments in an organized manner to facilitate the next use.
- The participant may change clothes after the removal of all equipment.

C.9 Enjoyment Assessment (3 min)

At the end of each session, participants completed the PACES-8 questionnaire to evaluate their subjective perception of enjoyment and satisfaction during the training under the two auditory conditions.

EXPERIMENTAL SESSION

This chapter presents the schematic representation of one experimental session.

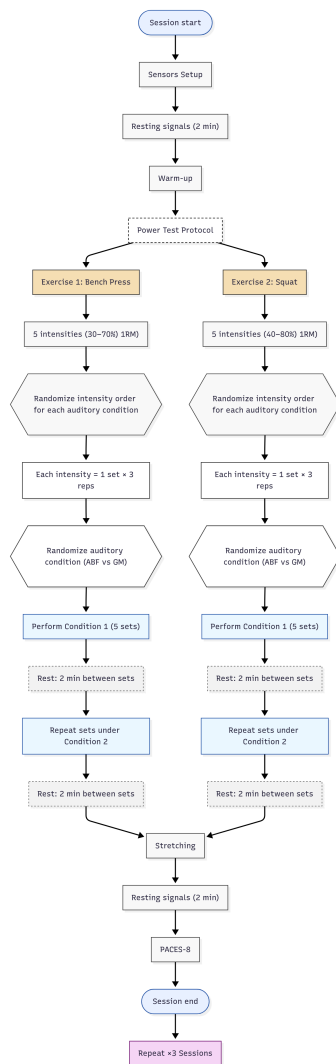


Figure D.1: Experimental Session.

EVENT DETECTION ALGORITHMS AND EMG PROCESSING

PROCESSING

This chapter presents the algorithms used for concentric phase detection, repetition onset and EMG processing.

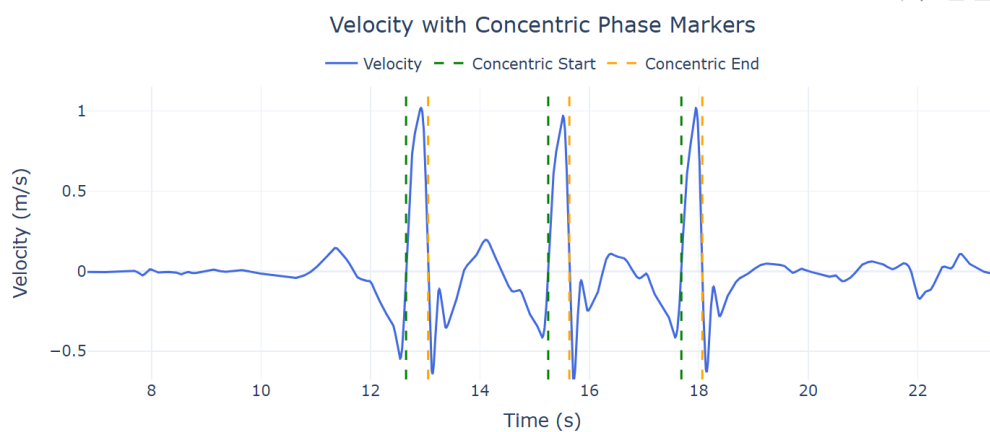


Figure E.1: Concentric Phase Detection Algorithm.

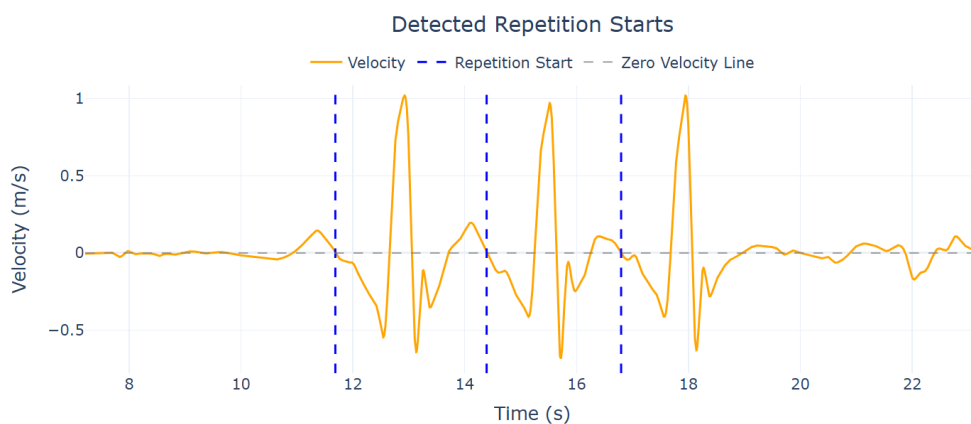


Figure E.2: Repetition Start Detection Algorithm.

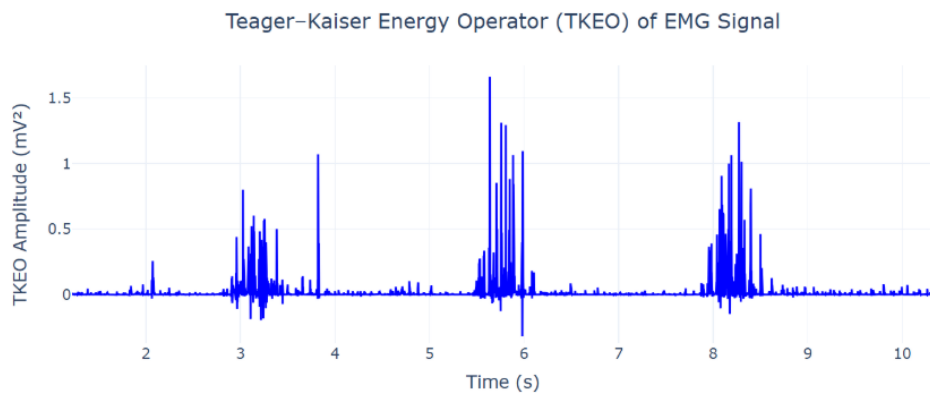


Figure E.3: Application of the Teager-Kaiser Energy Operator (TKEO).

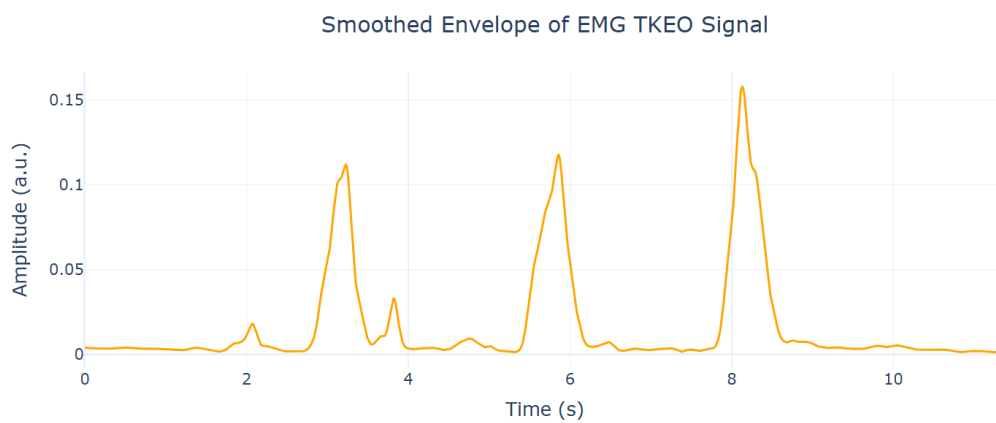


Figure E.4: Rectification and Gaussian smoothing used to obtain a stable EMG activation envelope.

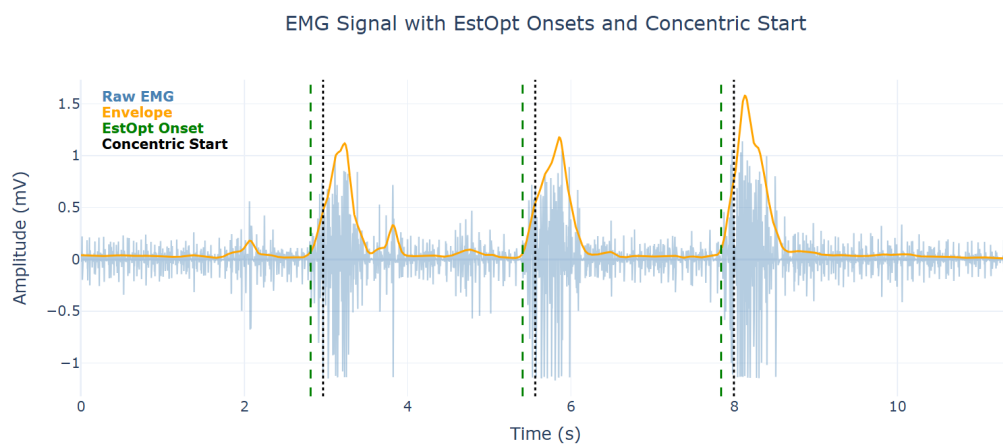


Figure E.5: EMG Onset Detection Algorithm.

SUPPLEMENTARY STATISTICAL TABLES

This chapter presents the extended statistical outputs obtained from JASP, including Bayesian repeated-measures ANOVA model comparisons.

Table F.1: Bayesian repeated-measures ANOVA model comparison for Maximum Power in the bench press (overall analysis).

Models	P(M)	P(M data)	BF_M	BF_{10}	error %
Sessions + Sex + Sessions * Sex	0.026	0.323	17.686	1.000	
Sessions + Sex + BM + Sessions * Sex	0.026	0.289	15.060	0.894	7.910
Sessions + Stimulus + Sex + Sessions * Sex	0.026	0.089	3.598	0.274	4.177
Sessions + Stimulus + Sex + BM + Sessions * Sex	0.026	0.072	2.889	0.224	6.192
Sessions + Stimulus + Sex + Sessions * Sex + Stimulus * Sex	0.026	0.031	1.179	0.096	5.011
Sessions + Stimulus + Sex + BM + Sessions * Sex + Stimulus * Sex	0.026	0.029	1.094	0.089	10.447
Sessions + Sex	0.026	0.026	0.996	0.081	3.900
Sessions + Stimulus + Sex + Sessions * Stimulus + Sessions * Sex	0.026	0.025	0.935	0.076	6.086
Sessions + Stimulus + Sex + BM + Sessions * Stimulus + Sessions * Sex	0.026	0.023	0.853	0.070	8.806
Sessions + Sex + BM	0.026	0.022	0.836	0.068	5.764

Legend: BM- Body Mass; P(M | data)- posterior model probability; BF_M - Bayes Factor comparing the best model to all others; $P(M)$ — prior model probability; BF_{10} — Bayes Factor comparing each model to the best-fitting model (odds of the model relative to the top model); "+" indicates inclusion of main effects; "*" indicates inclusion of the interaction between factors.

Table F.2: Bayesian repeated-measures ANOVA model comparison for Maximum Velocity in the bench press (overall analysis).

Models	P(M)	P(M data)	BF_M	BF_{10}	error %
Sessions + Sex + BM + Sessions * Sex	0.026	0.138	5.911	1.000	
Sessions + Sex + Sessions * Sex	0.026	0.136	5.826	0.988	7.339
Sessions + Stimulus + Sex + BM + Sessions * Sex	0.026	0.085	3.451	0.619	7.816
Sessions + Stimulus + Sex + Sessions * Sex	0.026	0.082	3.322	0.598	7.348
Sessions + Sex + BM	0.026	0.066	2.611	0.479	7.544
Sessions + Sex	0.026	0.063	2.488	0.457	7.168
Sessions + Stimulus + Sex + BM	0.026	0.043	1.660	0.312	10.752
Sessions + Stimulus + Sex + BM + Sessions * Sex + Stimulus * Sex	0.026	0.038	1.477	0.279	8.087
Sessions + Stimulus + Sex	0.026	0.038	1.450	0.274	7.267
Sessions + Stimulus + Sex + Sessions * Sex + Stimulus * Sex	0.026	0.036	1.374	0.260	7.360

Legend: BM- Body Mass; P(M | data)- posterior model probability; BF_M - Bayes Factor comparing the best model to all others; $P(M)$ — prior model probability; BF_{10} — Bayes Factor comparing each model to the best-fitting model (odds of the model relative to the top model); "+" indicates inclusion of main effects; "*" indicates inclusion of the interaction between factors.

Table F.3: Bayesian repeated-measures ANOVA model comparison for Peak RPD in the bench press (overall analysis).

Models	P(M)	P(M data)	BF _M	BF ₁₀	error %
Sessions + Sex + Sessions * Sex	0.026	0.115	4.820	1.000	
Sessions + Sex + BM + Sessions * Sex	0.026	0.109	4.548	0.950	12.180
Sex	0.026	0.106	4.374	0.917	10.209
Sex + BM	0.026	0.083	3.362	0.723	9.382
Sessions + Sex	0.026	0.069	2.728	0.596	8.655
Sessions + Sex + BM	0.026	0.062	2.443	0.537	10.580
Sessions + Stimulus + Sex + Sessions * Sex	0.026	0.048	1.856	0.415	8.993
Stimulus + Sex	0.026	0.042	1.606	0.361	8.677
Sessions + Stimulus + Sex + BM + Sessions * Sex	0.026	0.041	1.578	0.355	10.130
Stimulus + Sex + BM	0.026	0.038	1.473	0.332	10.525

Legend: BM- Body Mass; P(M|data)- posterior model probability; BF_M- Bayes Factor comparing the best model to all others; P(M) — prior model probability; BF₁₀ — Bayes Factor comparing each model to the best-fitting model (odds of the model relative to the top model); “+” indicates inclusion of main effects; “*” indicates inclusion of the interaction between factors.

Table F.4: Bayesian repeated-measures ANOVA model comparison for EMG Rise Time in the bench press (overall analysis).

Models	P(M)	P(M data)	BF _M	BF ₁₀	error %
Sessions + Sex + BM + Sessions * Sex	0.026	0.154	6.712	1.000	
Sessions + Sex + Sessions * Sex	0.026	0.148	6.425	0.964	5.854
Sessions + Stimulus + Sex + BM + Sessions * Sex	0.026	0.065	2.555	0.421	5.722
Sessions + Stimulus + Sex + Sessions * Sex	0.026	0.061	2.400	0.397	5.434
Sessions + BM	0.026	0.055	2.139	0.356	4.832
Sessions + Sex + BM	0.026	0.043	1.644	0.277	5.251
Sessions	0.026	0.041	1.598	0.270	4.145
Sessions + Sex	0.026	0.041	1.583	0.267	4.990
Wk_kg	0.026	0.032	1.214	0.207	4.802
Sessions + Stimulus + BM	0.026	0.026	0.972	0.167	4.851

Legend: BM- Body Mass; P(M|data)- posterior model probability; BF_M- Bayes Factor comparing the best model to all others; P(M) — prior model probability; BF₁₀ — Bayes Factor comparing each model to the best-fitting model (odds of the model relative to the top model); “+” indicates inclusion of main effects; “*” indicates inclusion of the interaction between factors.

Table F.5: Bayesian repeated-measures ANOVA model comparison for Maximum Power in the squat (overall analysis).

Models	P(M)	P(M data)	BF _M	BF ₁₀	error %
Sessions + Sex + BM + Sessions * Sex	0.026	0.336	18.720	1.000	
Sessions + Sex + Sessions * Sex	0.026	0.237	11.511	0.706	19.86
Sessions + Stimulus + Sex + BM + Sessions * Sex	0.026	0.093	3.807	0.278	20.24
Sessions + Stimulus + Sex + Sessions * Sex	0.026	0.089	3.609	0.265	19.83
Sessions + Stimulus + Sex + BM + Sessions * Sex + Stimulus * Sex	0.026	0.049	1.904	0.146	27.64
Sessions + Sex + BM	0.026	0.033	1.272	0.099	21.18
Sessions + Stimulus + Sex + Sessions * Sex + Stimulus * Sex	0.026	0.030	1.148	0.090	19.84
Sessions + Sex	0.026	0.024	0.898	0.071	19.78
Sessions + Stimulus + Sex + BM	0.026	0.022	0.846	0.067	40.93
Sessions + Stimulus + Sex + BM + Sessions * Stimulus + Sessions * Sex	0.026	0.021	0.779	0.061	22.47

Legend: BM- Body Mass; P(M|data)- posterior model probability; BF_M- Bayes Factor comparing the best model to all others; P(M) — prior model probability; BF₁₀ — Bayes Factor comparing each model to the best-fitting model (odds of the model relative to the top model); “+” indicates inclusion of main effects; “*” indicates inclusion of the interaction between factors.

APPENDIX F. SUPPLEMENTARY STATISTICAL TABLES

Table F.6: Bayesian repeated-measures ANOVA model comparison for Peak RPD in the squat (overall analysis).

Models	P(M)	P(M data)	BF _M	BF ₁₀	error %
Sessions + Sex + BM + Sessions * Sex	0.026	0.245	11.987	1.000	
Sessions + Sex + Sessions * Sex	0.026	0.164	7.277	0.672	19.27
Sessions + Stimulus + Sex + BM + Sessions * Sex	0.026	0.080	3.210	0.326	19.74
Sessions + Stimulus + Sex + Sessions * Sex	0.026	0.073	2.912	0.298	19.26
Sessions + Sex + BM	0.026	0.057	2.238	0.233	21.73
Sessions + Stimulus + Sex + BM	0.026	0.046	1.803	0.190	39.72
Sessions + Sex	0.026	0.045	1.752	0.185	19.19
Sessions + Stimulus + Sex + BM + Sessions * Sex + Stimulus * Sex	0.026	0.043	1.648	0.174	24.78
Sessions + Stimulus + Sex + BM + Sessions * Stimulus + Sessions * Sex	0.026	0.027	1.028	0.110	22.43
Sessions + Stimulus + Sex + Sessions * Sex + Stimulus * Sex	0.026	0.027	1.015	0.109	19.27

Legend: BM- Body Mass; P(M|data)- posterior model probability; BF_M- Bayes Factor comparing the best model to all others; P(M) — prior model probability; BF₁₀ — Bayes Factor comparing each model to the best-fitting model (odds of the model relative to the top model); "+" indicates inclusion of main effects; "*" indicates inclusion of the interaction between factors.

Table F.7: Bayesian repeated-measures ANOVA model comparison for Power Peak Index in the squat (overall analysis).

Models	P(M)	P(M data)	BF _M	BF ₁₀	error %
Session + Sex	0.026	0.113	4.737	1.000	
Sex	0.026	0.106	4.364	0.930	2.577
Session + BM	0.026	0.079	3.189	0.699	2.649
Session	0.026	0.078	3.142	0.690	2.121
BM	0.026	0.078	3.125	0.686	3.202
Session + Sex + BM	0.026	0.075	3.012	0.663	3.452
Null model (incl. subject and random slopes)	0.026	0.073	2.893	0.639	1.941
Sex + BM	0.026	0.066	2.636	0.586	2.586
Session + Stimulus + Sex	0.026	0.033	1.280	0.295	2.915
Stimulus + Sex	0.026	0.031	1.175	0.271	2.810

Legend: BM- Body Mass; P(M|data)- posterior model probability; BF_M- Bayes Factor comparing the best model to all others; P(M) — prior model probability; BF₁₀ — Bayes Factor comparing each model to the best-fitting model (odds of the model relative to the top model); "+" indicates inclusion of main effects; "*" indicates inclusion of the interaction between factors.

Table F.8: Bayesian repeated-measures ANOVA model comparison for Maximum Power in the bench press (sex-specific analysis: men).

Models	P(M)	P(M data)	BF _M	BF ₁₀	error %
Sessions	0.100	0.319	4.217	1.000	
Sessions + PAL	0.100	0.261	3.173	0.817	3.617
Sessions + Stimulus	0.100	0.115	1.172	0.361	2.459
Sessions + Stimulus + PAL	0.100	0.099	0.990	0.311	3.901
Sessions + Stimulus + Sessions * Stimulus	0.100	0.050	0.475	0.157	3.381
Sessions + Stimulus + PAL + Sessions * Stimulus	0.100	0.047	0.447	0.148	6.133
Null model (incl. subject and random slopes)	0.100	0.040	0.379	0.127	1.681
PAL	0.100	0.040	0.373	0.125	4.571
Stimulus	0.100	0.015	0.136	0.047	2.357
Stimulus + PAL	0.100	0.013	0.122	0.042	2.711

Legend: PAL- Physical Activity Level; P(M|data)- posterior model probability; BF_M- Bayes Factor comparing the best model to all others; P(M) — prior model probability; BF₁₀ — Bayes Factor comparing each model to the best-fitting model (odds of the model relative to the top model); "+" indicates inclusion of main effects; "*" indicates inclusion of the interaction between factors.

Table F.9: Bayesian repeated-measures ANOVA model comparison for Maximum Velocity in the bench press (sex-specific analysis: men).

Models	P(M)	P(M data)	BF _M	BF ₁₀	error %
Sessions	0.100	0.273	3.381	1.000	
Sessions + PAL	0.100	0.178	1.943	0.650	1.556
Sessions + Stimulus	0.100	0.161	1.723	0.588	1.426
Sessions + Stimulus + PAL	0.100	0.108	1.093	0.396	2.214
Null model (incl. subject and random slopes)	0.100	0.086	0.842	0.313	0.833
PAL	0.100	0.057	0.546	0.210	2.941
Stimulus	0.100	0.049	0.469	0.181	1.448
Sessions + Stimulus + Sessions * Stimulus	0.100	0.034	0.317	0.125	1.960
Stimulus + PAL	0.100	0.032	0.293	0.115	1.779
Sessions + Stimulus + PAL + Sessions * Stimulus	0.100	0.023	0.208	0.083	2.959

Legend: PAL- Physical Activity Level; P(M | data)- posterior model probability; BF_M- Bayes Factor comparing the best model to all others; P(M) — prior model probability; BF₁₀ — Bayes Factor comparing each model to the best-fitting model (odds of the model relative to the top model); “+” indicates inclusion of main effects; “*” indicates inclusion of the interaction between factors.

Table F.10: Bayesian repeated-measures ANOVA model comparison for Maximum Power in the squat (sex-specific analysis: men).

Models	P(M)	P(M data)	BF _M	BF ₁₀	error %
Sessions	0.100	0.380	5.525	1.000	
Sessions + PAL	0.100	0.279	3.477	0.733	2.349
Sessions + Stimulus	0.100	0.139	1.454	0.366	2.300
Sessions + Stimulus + PAL	0.100	0.104	1.043	0.273	3.083
Sessions + Stimulus + Sessions * Stimulus	0.100	0.050	0.478	0.133	2.628
Sessions + Stimulus + PAL + Sessions * Stimulus	0.100	0.038	0.352	0.099	4.249
Null model (incl. subject and random slopes)	0.100	0.004	0.037	0.011	1.540
PAL	0.100	0.003	0.028	0.008	5.109
Stimulus	0.100	0.002	0.014	0.004	2.436
Stimulus + PAL	0.100	0.001	0.010	0.003	2.581

Legend: PAL- Physical Activity Level; P(M | data)- posterior model probability; BF_M- Bayes Factor comparing the best model to all others; P(M) — prior model probability; BF₁₀ — Bayes Factor comparing each model to the best-fitting model (odds of the model relative to the top model); “+” indicates inclusion of main effects; “*” indicates inclusion of the interaction between factors.

Table F.11: Bayesian repeated-measures ANOVA model comparison for Peak RPD in the squat (sex-specific analysis: men).

Models	P(M)	P(M data)	BF _M	BF ₁₀	error %
Sessions	0.100	0.364	5.144	1.000	
Sessions + PAL	0.100	0.255	3.077	0.701	2.335
Sessions + Stimulus	0.100	0.125	1.282	0.343	2.128
Sessions + Stimulus + PAL	0.100	0.090	0.894	0.248	2.794
Null model (incl. subject and random slopes)	0.100	0.044	0.417	0.122	1.395
Sessions + Stimulus + Sessions * Stimulus	0.100	0.036	0.340	0.100	2.756
PAL	0.100	0.033	0.307	0.091	4.775
Sessions + Stimulus + PAL + Sessions * Stimulus	0.100	0.027	0.247	0.073	4.539
Stimulus	0.100	0.015	0.141	0.042	2.039
Stimulus + PAL	0.100	0.011	0.098	0.030	2.305

Legend: PAL- Physical Activity Level; P(M | data)- posterior model probability; BF_M- Bayes Factor comparing the best model to all others; P(M) — prior model probability; BF₁₀ — Bayes Factor comparing each model to the best-fitting model (odds of the model relative to the top model); “+” indicates inclusion of main effects; “*” indicates inclusion of the interaction between factors.

Table F.12: Bayesian repeated-measures ANOVA model comparison for EMG rise time in the bench press (sex-specific analysis: women).

Models	P(M)	P(M data)	BF _M	BF ₁₀	error %
Sessions	0.100	0.388	5.701	1.000	
Sessions + PAL	0.100	0.251	3.018	0.647	1.944
Sessions + Stimulus	0.100	0.136	1.416	0.351	1.919
Sessions + Stimulus + PAL	0.100	0.091	0.897	0.234	2.527
Sessions + Stimulus + Sessions * Stimulus	0.100	0.038	0.355	0.098	2.390
Null model (incl. subject and random slopes)	0.100	0.032	0.293	0.081	1.215
Sessions + Stimulus + PAL + Sessions * Stimulus	0.100	0.025	0.235	0.065	3.481
PAL	0.100	0.021	0.197	0.055	2.812
Stimulus	0.100	0.011	0.101	0.029	1.925
Stimulus + PAL	0.100	0.007	0.065	0.019	1.972

Legend: PAL- Physical Activity Level; P(M | data)- posterior model probability; BF_M- Bayes Factor comparing the best model to all others; P(M) — prior model probability; BF₁₀ — Bayes Factor comparing each model to the best-fitting model (odds of the model relative to the top model); “+” indicates inclusion of main effects; “*” indicates inclusion of the interaction between factors.





2025 The Acute Effects of Acoustic Biofeedback on Muscle Power

Beatriz Guerin

